PERGAMON

International Journal of Solids and Structures 39 (2002) 6241–6271

INTERNATIONAL JOURNAL OF SOLIDS and STRUCTURES

www.elsevier.com/locate/ijsolstr

A new thermodynamically consistent continuum model for hardening plasticity coupled with damage

Loredana Contrafatto, Massimo Cuomo *

Department of Civil and Environmental Engineering, University of Catania, V.le A. Doria, 6—95125 Catania, Italy

Received 15 August 2000; received in revised form 25 July 2002

Abstract

A phenomenological model for hardening–softening elasto-plasticity coupled with damage is presented. Specific kinematic internal variables are used to describe the mechanical state of the system. These, in the hypothesis of infinitesimal changes of configuration, are partitioned in the sum of a reversible and an irreversible part. The constitutive equations, developed in the framework of the Generalised Standard Material Model, are derived for reversible processes from an internal energy functional, postulated as the sum of the deformation energy and of the hardening energy both coupled with damage, while for irreversible phenomena from a dissipation functional.

Performing duality transformations, the conjugated potentials of the complementary elastic energy and of the complementary dissipation are obtained. From the latter a generalised elastic domain in the extended space of stresses and thermodynamic forces is derived. The model, which is completely formulated in the space of actual stresses, is compared with other formulations based on the concept of effective stresses in the case of isotropic damage. It is observed that such models are consistent only for particular choices of the damage coupling. Finally, the predictions of the proposed model for some simple processes are analysed.

Keywords: Continuum damage mechanics; Coupled plasticity and damage; Actual stresses and strains

1. Introduction

Detailed constitutive theories have been formulated in the literature to reproduce significant non-linearity in the mechanical behaviour of many materials. Although micro-structural models exist to describe specific phenomena such as plastic slips, dislocation evolution, micro-defect coalescence, fracture propagation, void growth etc., the analysis of coupling effects involving several of these phenomena is based on phenomenological theories, which, in spite of some simplifications, provide a detailed description of many geometrically complex engineering problems.

* Corresponding author. Tel.: +39-95-7382263; fax: +39-95-7382297.
E-mail address: mcuomo@dica.unict.it (M. Cuomo).

0020-7683/02/$ - see front matter
PII: S0020-7683(02)00470-5

Nomenclature

State variables
Kinematic

ε strain tensor
α hardening internal variable
ω damage internal variable
s specific entropy
$\eta = (\varepsilon, \alpha, \omega)$ vector of mechanical kinematic variables

Dual static

σ stress tensor
χ hardening internal force
ζ damage internal force
T temperature
$\tau = (\sigma, \chi, \zeta)$ vector of mechanical static variables
$(\ )_e$ reversible component of the generic kinematic variable
$(\ )_p$ irreversible component of the generic kinematic variable
$(\dot{\ })$ rate of the generic variable
σ' deviator of the stress tensor
ε'_e deviator of the elastic strain tensor
$\hat{\sigma}$, $\hat{\chi}$ effective stress and thermodynamic force

Energy symbols

$e(\varepsilon_e, \alpha_e, \omega_e, s_e)$ specific internal energy
$f(\varepsilon_e, \alpha_e, \omega_e, s_e)$ specific Helmoltz free energy
$\phi(\varepsilon_e, \omega_e, s_e)$ deformation potential
$\psi(\alpha_e, \omega_e, s_e)$ hardening potential
$\hat{\phi}(\varepsilon_e, \omega_e, s_e)$ effective deformation potential
$\hat{\psi}(\alpha_e, \omega_e, s_e)$ effective hardening potential
$d(\dot{\varepsilon}_p, \dot{\alpha}_p, \dot{\omega}_p, \dot{s}_p)$ specific dissipation
$d^c(\sigma, \chi, \zeta, T)$ specific conjugated dissipation
P_{vi} internal virtual power
r specific internal heat production
q heat flux
ρ material density
γ dissipated heat power

Constitutive symbols

E elasticity tensor
H hardening tensor
M_1 effective stresses operator
M_2 effective hardening forces operator
E_0, G_0 initial Young and shear moduli
$K(\sigma, \chi, \zeta)$ generalised elastic domain
$\Omega(\omega_e)$ set of the admissible values of the damage variable ω_e
R^- set of non-positive real numbers

R^+	set of non-negative real numbers
$g(\tau)$	yield function
n	real exponent of isotropic damage law
p	real coupling damage parameter
λ	plastic multiplier
μ	penalty parameter

Object of this contribution is the analysis of a fully coupled phenomenological theory of plasticity with hardening and damage. Damage is phenomenologically understood as a degradation both of the elastic stiffness of the material (and, eventually, of its micro-structure) and of its strength. However, as it will be shown, the theory of damage can also include phenomena such as fracture evolution, as it has been recently suggested (Paas et al., 1993). The proposed model follows the phenomenological approach because the material behaviour is described through a suitable set of internal variables, whose relation to micro-mechanical processes is not exactly defined. Particularly, a subset of internal variables is considered responsible of the damage evolution. The nature of these variables is generally tensorial (Hansen and Schreyer, 1994; Zhu and Cescotto, 1995), although they can be reduced to scalar quantities if only isotropic damage is considered.

Coupling between damage and plasticity is usually introduced redefining the plastic relations for the so called effective stresses (Kachanov, 1958; Cordebois and Sidoroff, 1982; Krajcinovic, 1984; Lemaitre and Chaboche, 1985; Ju, 1989). Flow rules for the plastic strain rates are consequently obtained including the damage variable as a parameter, which, in turn, is determined through a specific evolution law independent of the plastic potential (Hansen and Schreyer, 1994; Simo and Ju, 1987; Klisinski and Mròz, 1988; Marotti de Sciarra, 1997). It is then needed to solve a parametric optimisation problem, whose convergence properties are strongly dependent on the form chosen for the two potentials. A different thermodynamical model has been recently formulated by Armero and Oller (2000); this uses a partition of the strain in elastic, plastic, plus damage components, and employs the damaged stiffness directly as damage internal variables.

In this paper a new phenomenological model for a class of elastic–plastic damaging materials, that deviates from those mentioned above is presented. The main characteristics of the proposed model are summarised in the following. The framework of the Generalised Standard Material Model (Germain, 1973; Halphen and Nguyen, 1975) is adopted, so that the model is defined through the specification of two functionals of the kinematic variables, ruling the reversible and irreversible phenomena respectively. A general scheme is developed, based on duality. All internal variables are consistently decomposed in a reversible and an irreversible component, the first being responsible for the stored internal energy, the second generating the internal dissipation. The second principle of thermodynamics is satisfied a priori thanks to the hypotheses introduced for the structure of the dissipation functional. Full coupling with damage is allowed both in the free energy and in the dissipation. Applying duality transformations (Rockafellar, 1970), conjugated potentials of the mechanical variables dual to the kinematic variables are obtained, resulting in the generalised complementary elastic energy and in the complementary dissipation functional. The latter one is of fundamental importance, since its differential yields the evolution laws for the rate of internal variables. According to the choice of the dissipation functional, and therefore of the generalised elastic domain, coupling between plasticity and damage can be easily modelled and various kinds of behaviour, such as hardening–softening transition, cohesive fracture-like behaviour, etc., can be recovered, with no need of introducing ad-hoc evolution laws.

Two major consequences of this approach are stressed. First, an unified format for the evolution laws of any internal variable is obtained, and they all derive from a single potential of the driving forces. Secondly, the model implies the existence of a single elastic domain in the extended space of the actual stresses and of the thermodynamic forces dual to the hardening and damage internal variables. A natural extension of Drucker's principle applies to the generalised elastic domain, so that the postulate of maximum dissipation is fulfilled. Therefore satisfaction of the evolution laws is obtained solving a single optimisation problem, which turns out to be a straightforward generalisation of the one used in perfect plasticity.

The main characteristics of the model are first introduced and discussed without specifying any particular form for the governing functionals nor for the internal variables. Subsequently, as an exemplification, a very simple isotropic damage model is introduced similar to the one proposed by Lemaitre (1996) and some peculiar features of this model are presented, underlying the differences with the traditional damage models. It will be shown how the present proposal needs very few material constants, and that their experimental determination is based on the response of the material to simple fundamental tests. This result is due to the derivation of the coupled model from properly defined thermodynamic potentials, so that the constitutive evolution laws are not postulated but derived as a consequence of energy balances. The paper is concluded by an application to a structural problem.

As any damage/softening local model, also the proposed one suffers for the strain localisation problem, due to the loss of ellipticity of the tangent operator. Some of the strategies that have been presented in the literature to overcome this problem can be easily adapted to the proposed model, but the matter is beyond the scopes and the limits of the present paper.

2. Constitutive model

2.1. State variables and ambient spaces

A simple material is considered and the constitutive relations are developed within the framework of the Generalised Standard Material Model (Germain, 1973; Halphen and Nguyen, 1975). The assumption of local state is kept valid, i.e. the equilibrium state of a material point is assumed independent of the state of the neighbouring elements. The state of the system is phenomenologically described assigning a set of internal variables and the related mechanisms for energy exchange, distinguishing the reversible phenomena that modify the stored energy and the irreversible ones that cause energy dissipation.

The following kinematic variables and the associated dual mechanic variables, which are defined in the adjoint spaces (denoted by a prime), are considered:

$$\begin{array}{ll} \varepsilon \in D & \text{macroscopic strain} \\ \sigma \in D' & \text{stress} \\ \alpha \in I & \text{hardening} \\ \chi \in I' & \text{hardening internal forces} \\ \omega \in C & \text{damage} \\ \zeta \in C' & \text{damage driving forces} \\ s \in R & \text{entropy} \\ T \in R & \text{temperature} \end{array} \tag{1}$$

Besides the deformation ε, two sets of internal variables are introduced, acting at the micro-structural level: the variables α which describe the hardening mechanisms and the variables ω which measure the degradation of the material integrity and account for the decay of the elastic and hardening stiffness and of the strength of the material. Although some physical interpretation is possible, no link of these variables to any mechanism is attempted, leaving it to a specific implementation of the general model.

To each pair of conjugated variables a duality product is associated, which generates the following bilinear form of the internal virtual power:

$$P_{\mathrm{vi}} = \langle \sigma, \dot{\varepsilon} \rangle + \langle \chi, \dot{\alpha} \rangle + \langle \zeta, \dot{\omega} \rangle + \langle T, \dot{s} \rangle \tag{2}$$

The last term in (2) represents the heat exchange while the other terms correspond to the mechanical power. A superimposed dot denotes rates, and the scalar products in (2) are the appropriate ones to each pair. When necessary the whole sets of mechanical dual variables will be denoted by the symbols:

$$\begin{aligned} \eta &= (\varepsilon, \alpha, \omega) \\ \tau &= (\sigma, \chi, \zeta) \end{aligned} \tag{3}$$

In the paper only linear kinematic relations are considered (infinitesimal deformation), so that each kinematic variable is additively decomposed in a reversible and an irreversible component:

$$\begin{aligned} \varepsilon &= \varepsilon_{\mathrm{e}} + \varepsilon_{\mathrm{p}} \\ \alpha &= \alpha_{\mathrm{e}} + \alpha_{\mathrm{p}} = 0 \\ \omega &= \omega_{\mathrm{e}} + \omega_{\mathrm{p}} = 0 \\ s &= s_{\mathrm{e}} + s_{\mathrm{p}} \end{aligned} \tag{4}$$

Since for any closed system the power of the internal variables α, ω must be zero, their total value vanishes, i.e. their elastic and plastic parts are opposite (Kluitenberg, 1962; Ziegler, 1977).

According to the Generalised Standard Material Model, the constitutive relations are fully defined through the choice of the specific internal energy functional e and of the specific dissipation functional d, which depend on the local values of the kinematic variables:

$$e = e(\varepsilon_{\mathrm{e}}, \alpha_{\mathrm{e}}, \omega_{\mathrm{e}}, s_{\mathrm{e}}) \quad d = d(\dot{\varepsilon}_{\mathrm{p}}, \dot{\alpha}_{\mathrm{p}}, \dot{\omega}_{\mathrm{p}}, \dot{s}_{\mathrm{p}}) \tag{5}$$

2.2. Internal energy functional

The internal energy, dependent only on the reversible part of the kinematic variables, is postulated as the sum of a deformation energy $\phi(\varepsilon_{\mathrm{e}}, \omega_{\mathrm{e}}, s_{\mathrm{e}})$ and of a hardening energy $\psi(\alpha_{\mathrm{e}}, \omega_{\mathrm{e}}, s_{\mathrm{e}})$ coupled with damage:

$$e(\varepsilon_{\mathrm{e}}, \alpha_{\mathrm{e}}, \omega_{\mathrm{e}}, s_{\mathrm{e}}) = \phi(\varepsilon_{\mathrm{e}}, \omega_{\mathrm{e}}, s_{\mathrm{e}}) + \psi(\alpha_{\mathrm{e}}, \omega_{\mathrm{e}}, s_{\mathrm{e}}) + \mathrm{In}\,\Omega(\omega_{\mathrm{e}}) \tag{6}$$

The last term in (6) accounts for the unilateral nature of damage, being "$\mathrm{In}\,\Omega$" the convex indicator function of the set Ω of the possible values of the damage variable ($\mathrm{In}\,\Omega(\omega_{\mathrm{e}}) = 0$ if $\omega_{\mathrm{e}} \in \Omega$, $\mathrm{In}\,\Omega(\omega_{\mathrm{e}}) = +\infty$ if $\omega_{\mathrm{e}} \notin \Omega$). When ω_{e} reaches the boundary of Ω the material element is fully damaged. The model thus describes both the degradation of the elastic stiffness and of the hardening modulus.

From standard thermodynamic arguments, the constitutive relations for the dual static variables are obtained as elements of the sub-differentials of e (see Appendix A for the definition of sub-differential):

$$\begin{aligned} \sigma &\in \partial_{\varepsilon_{\mathrm{e}}}\phi \subset D' \\ \chi &\in \partial_{\alpha_{\mathrm{e}}}\psi \subset I' \\ \zeta &\in \partial_{\omega_{\mathrm{e}}}(\phi + \psi) \subset C' \\ T &\in \partial_{s_{\mathrm{e}}}(\phi + \psi) \in R \end{aligned} \tag{7}$$

In the sequel, as isothermal processes are considered, the dependence on entropy or temperature will be dropped.

In the context of the kinematic linear theory the deformation and the hardening potentials take the quadratic forms (a dot denotes the scalar product between 2nd order tensors):

$$\begin{aligned} \phi &= \frac{1}{2} E(\omega_{\mathrm{e}}) \varepsilon_{\mathrm{e}} \cdot \varepsilon_{\mathrm{e}} \quad E(0) = E_0 \\ \psi &= \frac{1}{2} H(\omega_{\mathrm{e}}) \alpha_{\mathrm{e}} \cdot \alpha_{\mathrm{e}} \quad H(0) = H_0 \end{aligned} \tag{8}$$

so that for a virgin material, $\omega_e = 0$ and the undamaged elastic and hardening moduli are recovered. The potential ϕ is convex in ε_e but globally not convex. Furthermore, the function $E(\omega_e)$ can be assumed convex in ω_e.

The form (8) has been often used in mechanics, and is based on the idea of the "effective stress" $\hat{\sigma}$, first proposed by Kachanov (1958). This is the stress that would be applied to an element of undamaged material so that it presents the same strain or the same elastic energy as the damaged element subjected to the current stress σ.

Indeed, employing the principle of equivalent elastic energy introduced by Cordebois and Sidoroff (1982), that states the equalities

$$\begin{aligned}\phi(\varepsilon_e, \omega_e) &= \hat{\phi}(\hat{\varepsilon}_e, 0)\\ \psi(\alpha_e, \omega_e) &= \hat{\psi}(\hat{\alpha}_e, 0)\end{aligned} \tag{9}$$

and defining the effective deformation operator such that $\hat{\varepsilon}_e = M_1^{-T}\varepsilon_e$ and $\hat{\alpha}_e = M_2^{-T}\alpha_e$, the expressions for the damaged stiffness and hardening tensors are:

$$\begin{aligned}E(\omega_e) &= M_1^{-1}E_0M_1^{-T}\\ H(\omega_e) &= M_2^{-1}H_0M_2^{-T}\end{aligned} \tag{10}$$

The constitutive equations (7) yield:

$$\begin{aligned}\sigma &= M_1^{-1}E_0M_1^{-T}\varepsilon_e\\ \chi &= M_2^{-1}H_0M_2^{-T}\alpha_e\end{aligned} \tag{11}$$

and in the effective spaces it holds:

$$\begin{aligned}\hat{\sigma} &= M_1\sigma = E_0M_1^{-T}\varepsilon_e = E_0\hat{\varepsilon}_e\\ \hat{\chi} &= M_2\chi = H_0M_2^{-T}\alpha_e = H_0\hat{\alpha}_e\end{aligned} \tag{12}$$

The operators M_1, M_2 are in general fourth order tensor (Hansen and Schreyer, 1994).

In this paper the concept of effective stress is not used. In order to simplify the analysis, only the case of isotropic damage is considered. The elastic potentials that constitute the internal energy are written as:

$$\phi(\varepsilon_e, \omega_e) = \frac{1}{2}E_0\varepsilon_e \cdot \varepsilon_e(1 + \omega_e)^n \tag{13}$$

$$\begin{aligned}\psi(\alpha_e, \omega_e) &= \frac{1}{2}H_0y(\omega_e)\alpha_e \cdot \alpha_e\\ \Omega &= \{\omega_e | -1 \leqslant \omega_e \leqslant 0\}\end{aligned} \tag{14}$$

with $n \geqslant 1$. The function y in (14) introduces a decay of the hardening modulus H_0. Different choices for it are possible. In the paper the following expression is used:

$$y(\omega_e) = p(1 + \omega_e)^n \quad p \in R \quad p \geqslant 0 \tag{15}$$

For $p = 0$ no coupling effect is present. Recall that from (4) it is:

$$\omega_e = -\omega_p \tag{16}$$

The function ϕ defined in Eq. (13) is convex in ε_e, ω_e for any $n \geqslant 1$ while is not globally convex as can be easily checked taking for instance the convex combination of the points:

$$\eta_1 \equiv (\bar{\varepsilon}_e, 0, \bar{\omega}_e) \quad \eta_2 \equiv \left(2\bar{\varepsilon}_e, 0, \frac{1}{2}\bar{\omega}_e\right)$$

for which it results, in the intermediate point $\eta_c = (1-\theta)\eta_1 + \theta\eta_2$:

$$\phi(\eta_c) \geqslant (1-\theta)\phi(\eta_1) + \theta\phi(\eta_2) \quad \forall\theta \in [0,1]$$

Graphically this is evident from Fig. 1, that shows the elastic potential and its level sets in the space of the variables ε_{e_1}, ω_e in an uniaxial case. Similar properties are true for the potential ψ, that, however, can be either convex or concave on α_e; in the latter case initial softening is obtained.

The generalised elastic relations, derived from definitions (13) and (14), become:

$$\begin{aligned} \sigma &= E_0\varepsilon_e(1+\omega_e)^n \\ \chi &= H_0\alpha_e p(1+\omega_e)^n \\ \zeta &= \frac{n}{2}E_0\varepsilon_e\cdot\varepsilon_e(1+\omega_e)^{n-1} + \frac{n}{2}pH_0\alpha_e\cdot\alpha_e(1+\omega_e)^{n-1} + \partial_{\omega_e}\mathrm{In}\,\Omega(\omega_e) \end{aligned} \tag{17}$$

The sub-differential of the indicator function that appears in the expression of ζ in (17) is known to coincide with the cone of the outward normals to the admissible domain Ω (Rockafellar, 1970). More specifically, since $\Omega = \{\omega_e | \omega_e \in R^-, (1+\omega_e) \in R^+\}$ being R^-, R^+ respectively the axes of the non-positive and non-negative real numbers,

$$\partial_{\omega_e}\mathrm{In}\,\Omega(\omega_e) = \zeta_{a_1} - \zeta_{a_2} \quad \zeta_{a1} \in \partial\,\mathrm{In}\,R^-(\omega_e) \quad \zeta_{a2} \in \partial\,\mathrm{In}\,R^+(1+\omega_e)$$

that is

$$\zeta_{a_1} \geqslant 0 \quad \omega_e \leqslant 0 \quad \zeta_{a_1}\omega_e = 0 \quad \zeta_{a_2} \leqslant 0 \quad (1+\omega_e) \geqslant 0 \quad \zeta_{a_2}(1+\omega_e) = 0$$

The inverse relations are, for $p \neq 0$:

$$\varepsilon_e = \frac{E_0^{-1}\sigma}{\left[\frac{n}{2(\zeta+\zeta_{a2}-\zeta_{a1})}\left(E_0^{-1}\sigma\cdot\sigma + \frac{1}{p}H_0^{-1}\chi\cdot\chi\right)\right]^{\frac{n}{1+n}}} \tag{18a}$$

$$\alpha_e = \frac{\frac{1}{p}H_0^{-1}\chi}{\left[\frac{n}{2(\zeta+\zeta_{a2}-\zeta_{a1})}\left(E_0^{-1}\sigma\cdot\sigma + \frac{1}{p}H_0^{-1}\chi\cdot\chi\right)\right]^{\frac{n}{1+n}}} \tag{18b}$$

$$1+\omega_e = \left[\frac{n}{2(\zeta+\zeta_{a2}-\zeta_{a1})}\left(E_0^{-1}\sigma\cdot\sigma + \frac{1}{p}H_0^{-1}\chi\cdot\chi\right)\right]^{\frac{1}{1+n}} \tag{18c}$$

In the rest of the paper p has been set equal to 1 for simplicity.

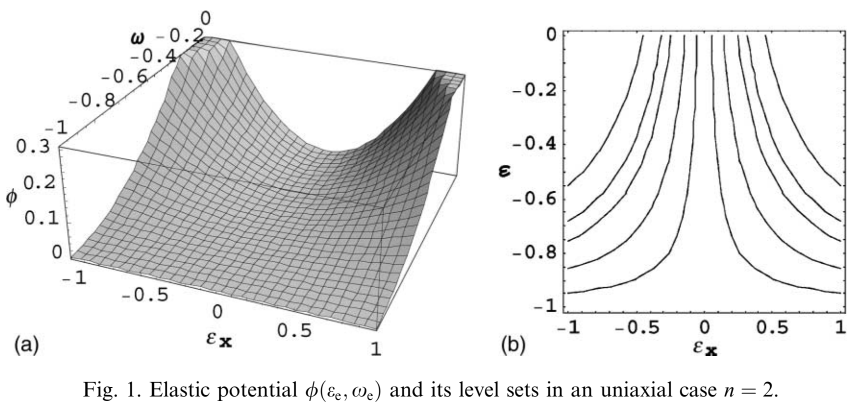

Fig. 1. Elastic potential $\phi(\varepsilon_e, \omega_e)$ and its level sets in an uniaxial case $n = 2$.

The complementary (Gibbs) free energy is obtained from (13) and (14) applying Legendre's transformation:

$$e^{c}(\sigma,\chi,\zeta)=\{\sigma\cdot\varepsilon_{e}+\chi\cdot\alpha_{e}+\zeta\cdot\omega_{e}-\phi(\varepsilon_{e},\omega_{e})-\psi(\alpha_{e},\omega_{e})-\text{In}\,\Omega\} \tag{19}$$

where the kinematic variables are related to the conjugated forces through the elastic relations (18a)–(18c).

A direct evaluation, substituting formulas (18a)–(18c) in (19), yields:

$$e^{c}(\sigma,\chi,\zeta)=\begin{cases} a_n\left(E_0^{-1}\sigma\cdot\sigma+\frac{1}{p}H_0^{-1}\chi\cdot\chi\right)^{\frac{1}{1+n}}\zeta^{\frac{n}{1+n}}-\zeta=e_1^{c} & \text{if } \zeta\geqslant\frac{n}{2}\left(E_0^{-1}\sigma\cdot\sigma+\frac{1}{p}H_0^{-1}\chi\cdot\chi\right)\\ \frac{1}{2}\left(E_0^{-1}\sigma\cdot\sigma+\frac{1}{p}H_0^{-1}\chi\cdot\chi\right) & \text{if } \zeta<\frac{n}{2}\left(E_0^{-1}\sigma\cdot\sigma+\frac{1}{p}H_0^{-1}\chi\cdot\chi\right)\end{cases}$$
$$a_n=\frac{1+n}{n}\left(\frac{n}{2}\right)^{\frac{1}{1+n}}\quad \zeta\geqslant 0 \tag{20}$$

The threshold value of ζ corresponds to a non-damaged situation ($\omega_e=0$), as it can be found substituting in Eqs. (18a)–(18c). Fig. 2 shows a section of the surface (20) with the ζ-axis for $\chi=0$ and constant uniaxial stress levels in the case $n=2$. For increasing ζ, the slope of the diagram decreases from the initial zero value.

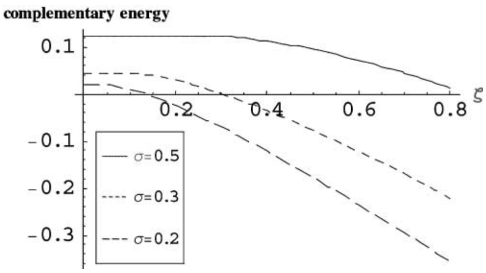

Fig. 2. Complementary energy functional in an uniaxial stress state. Section with planes $\sigma_1=\text{const}$, $n=2$.

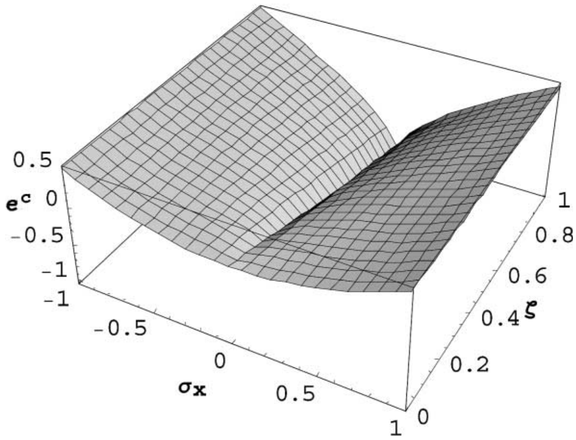

Fig. 3. Complementary energy functional in an uniaxial stress state, $n=2$.

The plot of e^c as a function of (σ_1, ζ) in Fig. 3 evidences its non-convexity. For $n = 1$, $n = 2$, it is:

$$\begin{aligned} e_1^c(\sigma, \chi, \zeta) &= \sqrt{2}\left(E_0^{-1}\sigma \cdot \sigma + \frac{1}{p}H_0^{-1}\chi \cdot \chi\right)^{1/2}\zeta^{1/2} - \zeta \quad n = 1 \\ e_1^c(\sigma, \chi, \zeta) &= \frac{3}{2}\left(E_0^{-1}\sigma \cdot \sigma + \frac{1}{p}H_0^{-1}\chi \cdot \chi\right)^{1/3}\zeta^{2/3} - \zeta \quad n = 2 \end{aligned} \tag{21}$$

2.3. The dissipation functional

The irreversible behaviour is ruled by the dissipation potential d, that has to comply with the second principle of thermodynamics, stating the irreversibility of entropy production (Chaboche, 1999):

$$\rho\dot{s} + \operatorname{div}\frac{q}{T} - \frac{r}{T} \geqslant 0 \tag{22}$$

where ρ is the material density, r the density of the internal heat production and q the heat flux for unit area. Introducing the first principle of thermodynamics for eliminating radiation r it is found:

$$\rho\dot{s} + \operatorname{div}\frac{q}{T} - \frac{1}{T}(\dot{e} - \sigma \cdot \dot{\varepsilon} - \chi \cdot \dot{\alpha} - \zeta \cdot \dot{\omega} + \operatorname{div} q) = \frac{1}{T}\left(\rho T\dot{s} - \dot{e} + \sigma \cdot \dot{\varepsilon} + \chi \cdot \dot{\alpha} + \zeta \cdot \dot{\omega} - q \cdot \frac{\operatorname{grad} T}{T}\right) \geqslant 0 \tag{23}$$

Inequality (23) transforms into the Clausius–Duhem inequality by means of the Helmoltz free energy $f = e - \rho Ts$, obtained from a Legendre transformation of the internal energy e, using the conjugate pair (s, T):

$$\gamma = \sigma \cdot \dot{\varepsilon} + \chi \cdot \dot{\alpha} + \zeta \cdot \dot{\omega} - (\dot{f} + \rho\dot{T}s) - q \cdot \frac{\operatorname{grad} T}{T} \geqslant 0 \tag{24}$$

where γ is the heat power dissipated by the material element during the plastic-damage process.

Under the classical hypothesis that f is constant w.r.t. the plastic components (Kluitenberg, 1962; Besseling and Van der Giessen, 1994), and observing that

$$\dot{f} = \frac{\partial f}{\partial \varepsilon_e}\dot{\varepsilon}_e + \frac{\partial f}{\partial \alpha_e}\dot{\alpha}_e + \frac{\partial f}{\partial \omega_e}\dot{\omega}_e + \frac{\partial f}{\partial T}\dot{T} = \sigma \cdot \dot{\varepsilon}_e + \chi \cdot \dot{\alpha}_e + \zeta \cdot \dot{\omega}_e - \rho s\dot{T} \tag{25}$$

the entropy production (24) becomes, using (4):

$$\gamma = \sigma \cdot \dot{\varepsilon}_p + \chi \cdot \dot{\alpha}_p + \zeta \cdot \dot{\omega}_p - \frac{q}{T} \cdot \operatorname{grad} T \geqslant 0 \tag{26}$$

In the case the mechanical dissipation is not coupled with the thermal dissipation, the following inequalities are separately satisfied:

$$\tau \cdot \dot{\eta}_p = \sigma \cdot \dot{\varepsilon}_p + \chi \cdot \dot{\alpha}_p + \zeta \cdot \dot{\omega}_p \geqslant 0 \quad -\frac{q}{T} \cdot \operatorname{grad} T \geqslant 0 \tag{27}$$

In the sequel, as isothermal processes will be considered, thermal dissipation will be neglected.

According to the Generalised Standard Material Model, the existence of a mechanical dissipation functional of the irreversible strain rates is now postulated, with the following properties:

- d is convex, proper, lower semi continuous;
- $d \ : D \times I \times C \to R \cup \{+\infty\} : \begin{cases} d(0) = 0 \\ d(\dot{\eta}_p) \geqslant 0 \quad \forall \dot{\eta}_p \neq 0 \end{cases}$ (28)
- d is such that $\tau \in \partial d(\dot{\eta}_p)$

Such a function automatically satisfies the reduced dissipation inequality (27) first part, as can be seen applying the definition of sub-differential:

$$\tau \in \partial d(\dot{\eta}_{\rm p}) = \left\{\tau | \tau \cdot (\bar{\dot{\eta}}_{\rm p} - \dot{\eta}_{\rm p}) \leqslant d(\bar{\dot{\eta}}_{\rm p}) - d(\dot{\eta}_{\rm p}) \quad \forall \bar{\dot{\eta}}_{\rm p}\right\} \tag{29}$$

Taking $\bar{\dot{\eta}}_{\rm p} = 0$ from (29) it follows

$$\tau \in \partial d(\dot{\eta}_{\rm p}) \iff \tau \cdot \dot{\eta}_{\rm p} \geqslant d(\dot{\eta}_{\rm p}) \geqslant 0 \tag{30}$$

If it is made the additional hypothesis that d is positively homogeneous, then from inequality (29), choosing once $\bar{\dot{\eta}}_{\rm p} = \theta\dot{\eta}_{\rm p}$, then $\bar{\dot{\eta}}_{\rm p} = -\theta\dot{\eta}_{\rm p}$, $\theta > 1$, it is found that

$$\left.\begin{array}{c}\tau \in \partial d(\dot{\eta}_{\rm p}) \\ d \text{ pos hom}\end{array}\right\} \Rightarrow d(\dot{\eta}_{\rm p}) = \tau \cdot \dot{\eta}_{\rm p} \tag{31}$$

Since $\partial d(0) = \{\tau \in D' \times I' \times C' | \tau \cdot \bar{\dot{\eta}}_{\rm p} \leqslant d(\bar{\dot{\eta}}_{\rm p}) \quad \forall \bar{\dot{\eta}}_{\rm p}\}$, it follows that all admissible internal forces τ given by (29) belong to the convex closed set $\partial d(0)$:

$$\tau \in \partial d(\dot{\eta}_{\rm p}) \subset \partial d(0) = K \quad \forall \dot{\eta}_{\rm p} \tag{32}$$

This is demonstrated as follows:

$$\tau \in \partial d(\dot{\eta}_{\rm p}) \Rightarrow \tau \cdot (\bar{\dot{\eta}}_{\rm p} - \dot{\eta}_{\rm p}) \leqslant d(\bar{\dot{\eta}}_{\rm p}) - d(\dot{\eta}_{\rm p}) \quad \forall \bar{\dot{\eta}}_{\rm p} \Rightarrow \tau \cdot \bar{\dot{\eta}}_{\rm p} \leqslant d(\bar{\dot{\eta}}_{\rm p}) \Rightarrow \tau \in \partial d(0)$$

The set K is then the generalised elastic domain in the space of all conjugated thermodynamic forces (see for a more accurate discussion Romano et al., 1993).

Since, by the definition (32) it is

$$K = \{\tau : \tau \cdot \dot{\eta}_{\rm p} \leqslant d(\dot{\eta}_{\rm p}), \quad \forall \dot{\eta}_{\rm p} \in D \times I \times C\} \tag{33}$$

it follows that the maximum dissipation principle holds:

$$d(\dot{\varepsilon}_{\rm p}, \dot{\alpha}_{\rm p}, \dot{\omega}_{\rm p}) = \sup_{(\sigma,\chi,\zeta)\in K} \{\sigma \cdot \dot{\varepsilon}_{\rm p} + \chi \cdot \dot{\alpha}_{\rm p} + \zeta \cdot \dot{\omega}_{\rm p}\} \tag{34}$$

The present model satisfies therefore Drucker's stability postulate in the space of the extended thermodynamic forces.

Eq. (34) implies that the dissipation functional is equal to the support function of the convex domain K (see Appendix A):

$$d(\dot{\eta}_{\rm p}) = \operatorname{supp} K \tag{35}$$

A standard theorem of convex analysis states than that the conjugated dissipation function is given by:

$$d^{\rm c}(\tau) = \sup_{\dot{\eta}_{\rm p}} \{\sigma \cdot \dot{\varepsilon}_{\rm p} + \chi \cdot \dot{\alpha}_{\rm p} + \zeta \cdot \dot{\omega}_{\rm p} - \operatorname{supp} K\} = \operatorname{In} K(\sigma, \chi, \zeta) \tag{36}$$

The conjugated potentials (35) and (36) satisfy Fenchel's inequality (Rockafellar, 1970)

$$\begin{aligned} & d(\dot{\eta}_{\rm p}) + d^{\rm c}(\tau) \leqslant \tau \cdot \dot{\eta}_{\rm p} \\ & d(\dot{\eta}_{\rm p}) + d^{\rm c}(\tau) = \tau \cdot \dot{\eta}_{\rm p} \iff \tau \in \partial d(\dot{\eta}_{\rm p}) \quad \dot{\eta}_{\rm p} \in \partial d^{\rm c}(\tau) \end{aligned} \tag{37}$$

the equality sign holding only for pairs of variable conjugated through the constitutive equations.

The flow rules for the rates of the irreversible strains are thus:

$$\dot{\eta}_{\rm p} \in \partial \operatorname{In} K(\tau) \tag{38}$$

Recalling that the sub-differential of the indicator function of the convex set K coincides with the cone of the outward normals to the set K, Eq. (38) generalises the normality condition for all the irreversible kinematic variables.

The presented model is therefore associative. An extended Drucker's stability criterion holds in the form:

$$(\tau_2 - \tau_1) \cdot \dot{\eta}_p \leqslant 0 \quad \forall \tau_1, \tau_2 \in K, \quad \forall \dot{\eta}_p \in \partial d^c(\tau_1) \tag{39}$$

In consideration of the equivalence (37) it is possible to characterise the irreversible behaviour of the model either specifying the dissipation functional or its conjugate. The latter way is usually simpler, since it is sufficient to define the elastic domain in the extended space of stresses, hardening forces and dual damage variables, by means of a convex yield function, assumed henceforth positively homogeneous:

$$K = \{(\sigma, \chi, \zeta) : g(\sigma, \chi, \zeta) \leqslant 0\} \tag{40}$$

The flow rules are then expressed as:

$$\dot{\eta}_p \in \lambda \partial_\tau g \quad \lambda \in \partial R^-[g] \tag{41}$$

The condition on the multiplier λ means that it satisfies the Kuhn-Tucker conditions:

$$\lambda g = 0 \quad \lambda \geqslant 0 \;\; g \leqslant 0 \tag{42}$$

The consistency condition $\lambda \dot{g} = 0$ must be added for structural analysis and this springs out naturally from the rate formulation of the constitutive equation (32) in a way totally identical to the case of perfect plasticity. The relevant developments can be found in Cuomo and Contrafatto (2000a).

More generally, the yield function is defined as

$$g = \sup\{g_i\} \quad i = 1, \ldots, n \tag{43}$$

and the admissible domain $K = \cap_{i=1,n} K_i$ is the convex hull of the limit surfaces. As a consequence in corner points more than one mechanism can be simultaneously active.

Remark 1. Thanks to its structure, the model can easily be extended to accommodate specific plastic-damage material behaviours. This can be done for instance including more than one damage internal variables, each one accounting for a different physical mechanism. As an example, such an approach has been used to model the different nature of damage exhibited by concrete-like materials in the tension and in the compression range (Cuomo and Contrafatto, 2000b). Furthermore, forms of the internal energy or of the dissipation potential different from those used in the paper can be applied, subjected only to the thermodynamic restrictions (28). For instance, time-dependent (viscous) damage plasticity can be obtained if a dissipation potential combination of positively homogeneous functions and of homogeneous functions of degree $n > 1$ is used (Cuomo, submitted for publication). Following the developments described in the quoted paper in place of (41) and (42) a Perzyna-type flow-rule is obtained,

$$\dot{\eta}_p = \mu g_+ \partial_\tau g \tag{44}$$

where μ is a real a viscosity parameter and $g_+ = \max\{g, 0\}$.

Multi-dissipation mechanisms can also be introduced, considering multi-surface elastic domains, as suggested in (43).

Remark 2. The form (17) of the generalised elastic relation recovers the one used by many authors (Simo and Ju, 1987; Ju, 1989). The coupled effect of damage on elastic stiffness and on the hardening moduli is apparent. Additional degrees of freedom can be obtained if the exponent n of the damage law is assumed to be different for the elastic and the plastic moduli. This is often needed for fitting experimental data and corresponds to the different evolution of damage in the texture of the material and in the mechanism of nucleation of defects.

3. The admissible domain

In paragraph 2 it has been shown that the maximum dissipation principle (34) implies the existence of an elastic domain K of the generalised stresses that can be described by means of the yield functional (43). Different definitions are encountered in literature. Aim of this paragraph is to examine and compare some of them with the present model.

In Lemaitre (1996), Lemaitre and Chaboche (1985), Borino et al. (1996) it is assumed that the maximum dissipation principle is satisfied separately for the stresses and the damage variables

$$\begin{aligned} d_1(\dot{\varepsilon}_\mathrm{p}, \dot{\alpha}_\mathrm{p}) &= \sup_{(\sigma,\chi)\in K_1} \{\sigma \cdot \dot{\varepsilon}_\mathrm{p} + \chi \cdot \dot{\alpha}_\mathrm{p}\} = \mathrm{supp}\, K_1(\dot{\varepsilon}_\mathrm{p}, \dot{\alpha}_\mathrm{p}) \\ d_2(\dot{\omega}_\mathrm{p}) &= \sup_{\zeta\in K_2}\{\zeta \cdot \dot{\omega}_\mathrm{p}\} = \mathrm{supp}\, K_2(\dot{\omega}_\mathrm{p}) \end{aligned} \tag{45}$$

Condition (45) is not equivalent to (34), being

$$\sup_{(\sigma,\chi,\zeta)\in K} \{\sigma \cdot \dot{\varepsilon}_\mathrm{p} + \chi \cdot \dot{\alpha}_\mathrm{p} + \zeta \cdot \dot{\omega}_\mathrm{p}\} \leqslant \sup_{(\sigma,\chi)\in K_1} \{\sigma \cdot \dot{\varepsilon}_\mathrm{p} + \chi \cdot \dot{\alpha}_\mathrm{p}\} + \sup_{\zeta\in K_2}\{\zeta \cdot \dot{\omega}_\mathrm{p}\} \tag{46}$$

As a consequence of (45) two different yield modes originate:

$$g_1(\sigma, \chi) \leqslant 0 \quad g_2(\zeta) \leqslant 0 \tag{47}$$

as opposite to (40). The situation is graphically represented in Fig. 4 with reference to the uniaxial case. Fig. 4 shows a sketch of the domain $C = \{\dot{\eta}_\mathrm{p} | d(\dot{\eta}_\mathrm{p}) \leqslant 1\}$, polar to K (Rockafellar, 1970; Romano et al., 1992), in the sense that $K = \{\tau | \langle \tau, \dot{\eta}_\mathrm{p}\rangle \leqslant 1 \quad \forall \dot{\eta}_\mathrm{p} \in C\}$. In the case that two uncoupled dissipation potentials are assumed as in (45) the domain C reduces to two segments on the coordinate axes, and similarly happens to the admissible domains K_1, K_2. Although they are convex in the relevant subspaces of $D' \times I' \times C'$ their intersection in not convex in the entire space of static variables.

According to our previous developments, adopting $d = d_1 + d_2$, as on the RHS of (46), the domains C and K with dashed borders are obtained. However, all the convex domains having their borders between the solid and the dashed lines in Fig. 4, corresponding to different choices of the dissipation d, are admissible. It is apparent that the proposed model permits a more accurate definition of the admissibility condition, allowing interaction effects between the stresses and the conjugated damage variables and ensuring convexity of the yield locus.

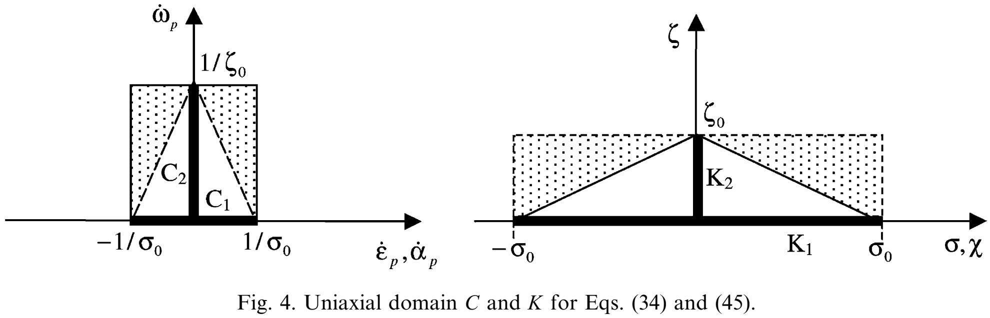

Fig. 4. Uniaxial domain C and K for Eqs. (34) and (45).

One more consequence of (45) is noticeable. The following flow rules correspond to the yield domains (47):

$$(\dot{\varepsilon}_p, \dot{\alpha}_p) \in \lambda_1 \partial_{(\sigma,\chi)} g_1(\sigma, \chi) \quad \dot{\omega}_p \in \lambda_2 \partial_\zeta g_2(\zeta) \tag{48}$$

Two distinct Lagrangian multipliers are thus introduced. On the contrary, in the case of Eq. (41), only one multiplier is needed, so that efficient algorithms can be used for overcoming the numerical difficulties at corner points (Bertsekas, 1982).

In the model proposed in Section 2 the yield functional is a function of the actual thermodynamic conjugated forces only. On the contrary, many authors account for damage coupling defining the yield function in the effective stress space (Lemaitre and Chaboche, 1985; Hansen and Schreyer, 1994; Marotti de Sciarra, 1997):

$$\hat{g} = \hat{g}(\hat{\sigma}, \hat{\chi}) \quad \hat{\sigma} = M\sigma \quad \hat{\chi} = M\chi \tag{49}$$

where $M = M(\omega_e)$ is the effective stress operator introduced in (9)–(12).

Usually the function $\hat{g}$ is assumed to be equal to the yield function of the undamaged material, so that

$$\hat{g}(\hat{\sigma}, \hat{\chi}) = g(\hat{\sigma}, \hat{\chi}) \tag{50}$$

Thus, in this case, the yield function is not fully defined in the space of conjugated thermodynamic forces and $g(\hat{\sigma}, \hat{\chi})$, which is convex in the effective force space, does not directly define the complementary dissipation potential (36).

In order to obtain the domain K in the space of the conjugated internal forces, the kinematic internal variable ω_e can be eliminated from (50) using the elastic constitutive relation:

$$g(\hat{\sigma}(\omega_e), \hat{\chi}(\omega_e)) = \tilde{g}(\sigma, \chi, \omega_e(\sigma, \chi, \zeta)) = \tilde{g}(\sigma, \chi, \zeta) \tag{51}$$

It is stressed that the convexity of g in the effective stress space does not guarantee the convexity of $\hat{g}$ in the space of actual internal forces.

For instance consider the expression of Mises criterion in a plane stress state without hardening in the effective stress space:

$$g(\hat{\sigma}) = \sqrt{3\hat{J}_2} - \sigma_0 \leqslant 0 \quad \hat{J}_2 = \frac{1}{2}\hat{\sigma}' \cdot \hat{\sigma}' \quad \hat{\sigma}' = \hat{\sigma} - \frac{1}{3}\mathrm{tr}(\hat{\sigma})I \quad \hat{\sigma} = M\sigma = \frac{\sigma}{(1+\omega_e)^n} \tag{52}$$

where a scalar form for M has been employed.

Introducing the expression (18c) for ω_e in the case $\chi = 0$, the following form of $\hat{g}$ is obtained:

$$\hat{g}(\sigma, \zeta) = \sqrt{\left(\frac{2\zeta}{n}\right)^{\frac{2n}{n+1}} \left(\frac{\sigma_x^2 - 2\nu\sigma_x\sigma_y + \sigma_y^2}{E_0}\right)^{-\frac{2n}{n+1}} (\sigma_x^2 - \sigma_x\sigma_y + \sigma_y^2)} - \sigma_0 \tag{53}$$

In Fig. 5 the surface (53) is represented in the space $(\sigma_x, \sigma_y, \zeta)$ and in Fig. 6 its level sets for a fixed value of ζ are shown using for the exponent n of the effective stress operator values between 1 and 2. Clearly, for whatever $n > 1$ the domain K is not convex.

The admissible domain (53) in the uniaxial case is examined in Fig. 7 where the undamaged elastic path for uniaxial stress is represented. Note that in the actual conjugated thermodynamic forces space it does not correspond neither to the stress axis, nor to a straight line.

However, it is noted that the domain (53) is convex in the space of actual strains, recovering in this case the Von Mises expression:

$$\tilde{g}(\varepsilon_e) = 2G_0\|\varepsilon_e'\| - \sigma_0 \quad \varepsilon_e' = \varepsilon_e - \frac{1}{3}\mathrm{tr}(\varepsilon_e)I \tag{54}$$

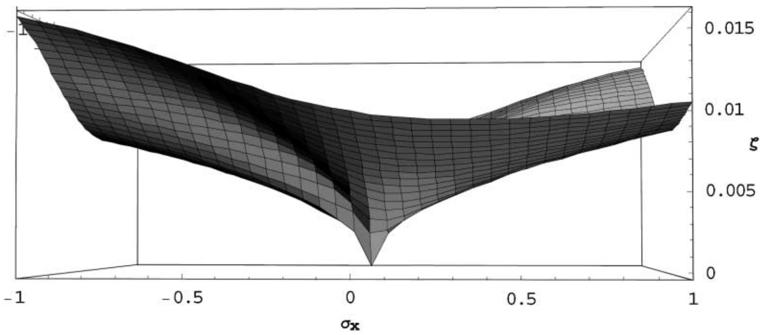

Fig. 5. Limit surface of function (53) $E_0 = 100$, $\sigma_0 = 1$, $n = 1.5$.

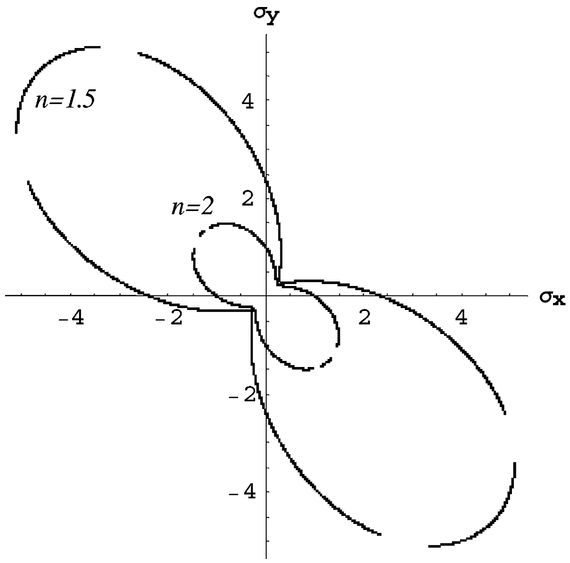

Fig. 6. Level sets of function (53) at $\zeta = 0.01$, $E_0 = 100$, $\sigma_0 = 1$, $n = 1.5, 2$.

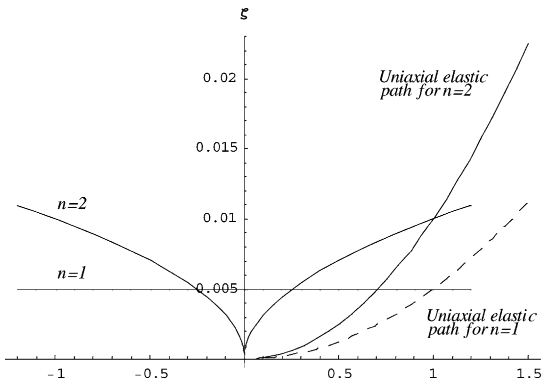

Fig. 7. Section of function (53) with the plane $\sigma_y = 0$ (uniaxial case).

It is also observed that, if an yield function of the type (50) is employed, the consistent flow rule (38) becomes:

$$\dot{\varepsilon}_{\mathrm{p}} \in \lambda\left[\partial_\sigma g + \partial_{\omega_{\mathrm{e}}} g \frac{\partial \omega_{\mathrm{e}}}{\partial \sigma}\right] = \lambda[\partial_\sigma g + \partial_{\omega_{\mathrm{e}}} g \nabla^2_{\zeta\sigma} e^{\mathrm{c}}(\sigma,\chi,\zeta)] \tag{55}$$

Therefore an extra term depending on the complementary elastic energy $e^{\mathrm{c}}(\sigma,\chi,\zeta)$ appears in the expression of the plastic strain rate. It vanishes only if $\nabla^2_{\zeta\sigma} e^{\mathrm{c}} = 0$, that is if $e^{\mathrm{c}}(\sigma,\chi,\zeta)$ is uncoupled in (σ,ζ), contrarily to the constitutive hypothesis.

4. Some models of coupled plasticity and damage

4.1. The case of isotropic damage

In this paragraph some properties of the model proposed in Section 2 are investigated using a dissipation mechanism produced by a single potential. In this context the model is characterised by a single plastic failure mode. A Mises-type and a Drucker-Prager-type criterion with hardening and damage are considered:

$$g_1(\sigma,\chi,\zeta) = \sqrt{3J_2} - (k_0 + \chi - c\zeta) \leqslant 0 \quad J_2 = \frac{1}{2}\sigma' \cdot \sigma' \quad c \in R^+ \quad k_0 = \sigma_0 + c\frac{n}{2}\frac{\sigma_0^2}{E_0} \tag{56}$$

$$g_2(\sigma,\chi,\zeta) = \sqrt{3J_2} + \frac{\beta}{3} I_1 - (k_0 + \chi - c\zeta) \leqslant 0 \quad I_1 = \mathrm{tr}(\sigma) \quad \beta, c, k_0 \in R^+ \tag{57a}$$

$$\beta = 3\frac{\xi - 1}{\xi + 1} + 3\frac{cn}{2E}\frac{|y_c|}{\xi}\frac{(\xi^2 - 1)}{(\xi + 1)} \quad k_0 = 2\frac{|y_c|}{\xi + 1} + \frac{cn}{2E}\frac{y_c^2}{\xi} \quad \xi = \frac{|y_c|}{y_t} \tag{57b}$$

where y_c and y_t are the compressive and tensile resistances, E_0 is the initial Young modulus and the parameter c rules the rate of damage. A damage fracture-type criterion is also considered, characterised by the function g_3:

$$g_3(\zeta) = \zeta - \zeta_0 \leqslant 0 \quad \zeta_0 \in R^+ \tag{58}$$

The functions g_1 and g_2 are the classical expressions of the Mises and Drucker-Prager criteria with the addition of two variables: the isotropic hardening variable χ, that rules the homothetic expansion of the plastic surface and the isotropic damage energy ζ, dual of the damage variable ω, that describes the contraction of the domain when damage is active. The rate of the contraction is ruled by the constitutive parameter c.

The function g_3 introduces a bound for the damage variable which is related to the fracture energy, as it will be better explained in Section 4.2. A functional dependency on the stresses can also be introduced to reproduce coupling phenomena of plasticity and fracture.

It is observed that the considered yield functions are all positively homogeneous, contrarily to the expressions obtained in the case an effective stress plastic criterion is used (see Eq. (53)). Dually, in opposition to the case (54), the form of the yield criterions (56), (57a), (57b), (58) in the space of actual kinematic variables is not positively homogeneous. For instance Mises criterion (56) provides:

$$g(\varepsilon_{\mathrm{e}},\alpha_{\mathrm{e}},\omega_{\mathrm{e}}) = (2G_0\|\varepsilon'_{\mathrm{e}}\| + H_0\alpha_{\mathrm{e}})(1+\omega_{\mathrm{e}})^n + c\frac{n}{2}(E_0\varepsilon_{\mathrm{e}}\cdot\varepsilon_{\mathrm{e}} + H_0\alpha_{\mathrm{e}}\cdot\alpha_{\mathrm{e}})(1+\omega_{\mathrm{e}})^{n-1} - k_0 \tag{59}$$

In any case expressions (56), (57a), (58), (59) are convex in the spaces of actual stresses or strains.

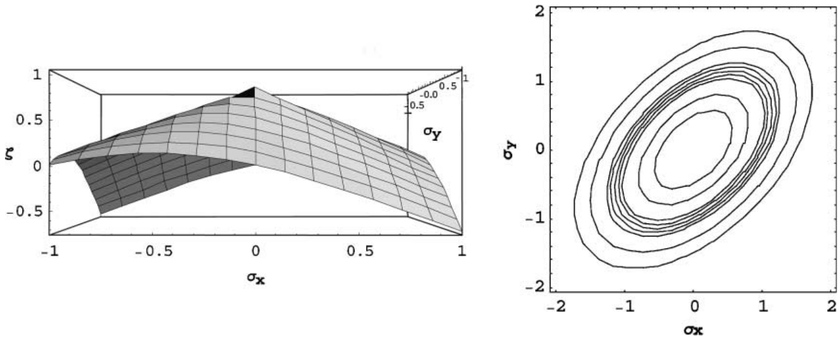

Fig. 8. Limit surface (56) and its level sets $\omega_e = \text{const}$, $E_0 = 100$, $\sigma_0 = 1$, $n = 2$.

A representation of the limit surface obtained from Eq. (56) in the space of the internal forces is shown in Fig. 8 for a plane stress state, together with its section with a plane $\zeta = \text{const}$. These figures have to be compared with Figs. 5 and 6.

The model is completed by the elastic relations Eq. (17). In addition to the usual elastic and hardening constants, only two new material parameters are introduced, namely the damage exponent n and the damage rate c.

4.2. Predictions of the model

The damage response of the model presented in Sections 2 and 4.1 is analysed considering some simple uniaxial processes.

The pure damage response obtained employing the fracture-type criterion (58) is examined first. The evolution of the damage variable ω_e in uniaxial extension is given by:

$$(1 + \omega_e) = \left(\frac{\varepsilon_0}{\varepsilon_e}\right)^{\frac{2}{n-1}} \quad \varepsilon_0 = \sqrt{\frac{2}{n}\frac{\zeta_0}{E_0}} \quad n > 1 \tag{60}$$

where ε_0 is the limit uniaxial elastic strain. Eq. (60) shows that ω_e tends asymptotically to -1 (corresponding to a fully damaged state). The stress follows from the elastic relation:

$$\sigma = E_0\left(\frac{\varepsilon_0^{2n}}{\varepsilon^{n+1}}\right)^{\frac{1}{n-1}} \quad n > 1 \tag{61}$$

The stress–strain curves are shown in Fig. 9 for different values of the parameter n. For $n = 1$ the limit case of instantaneous fracture is recovered. The loading–unloading behaviour is considered in Fig. 9b. It is noteworthy that the energy corresponding to a fully damaged state (that can be interpreted as fracture energy) is finite, in fact:

$$G_f = \int_0^{\varepsilon_0} \sigma \mathrm{d}\varepsilon + \int_{\varepsilon_0}^{\infty} \sigma \mathrm{d}\varepsilon = \frac{1}{2}E_0\varepsilon_0^2 + \frac{n-1}{2}E_0\varepsilon_0^2 = \frac{n}{2}E_0\varepsilon_0^2 = \zeta_0$$

Due to the presence of damage the application of this model to structural problems will cause strain localisation with the consequent mesh-dependency of the numerical results. Some regularisation is required, either in time or in space and several proposal can be found in literature. However, the aim of this paper is to introduce the model and the possible strategies for coping with strain localisation are beyond the goal of the present work.

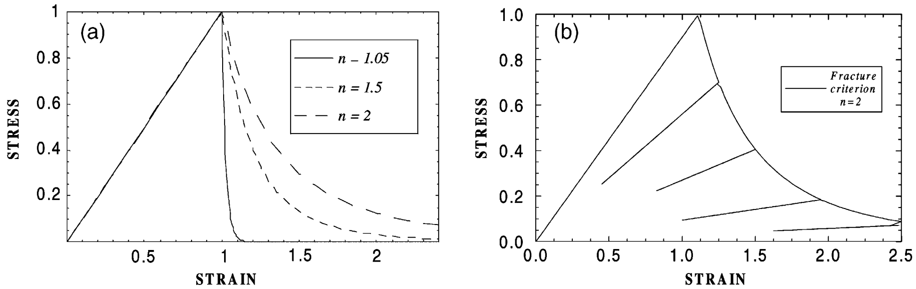

Fig. 9. (a, b) Fracture-type criterion. Influence of parameter n. Loading–unloading process.

The coupled plastic-damage models are examined in the sequel. The first set of results refers to Mises yield function g_1 of Eq. (56).

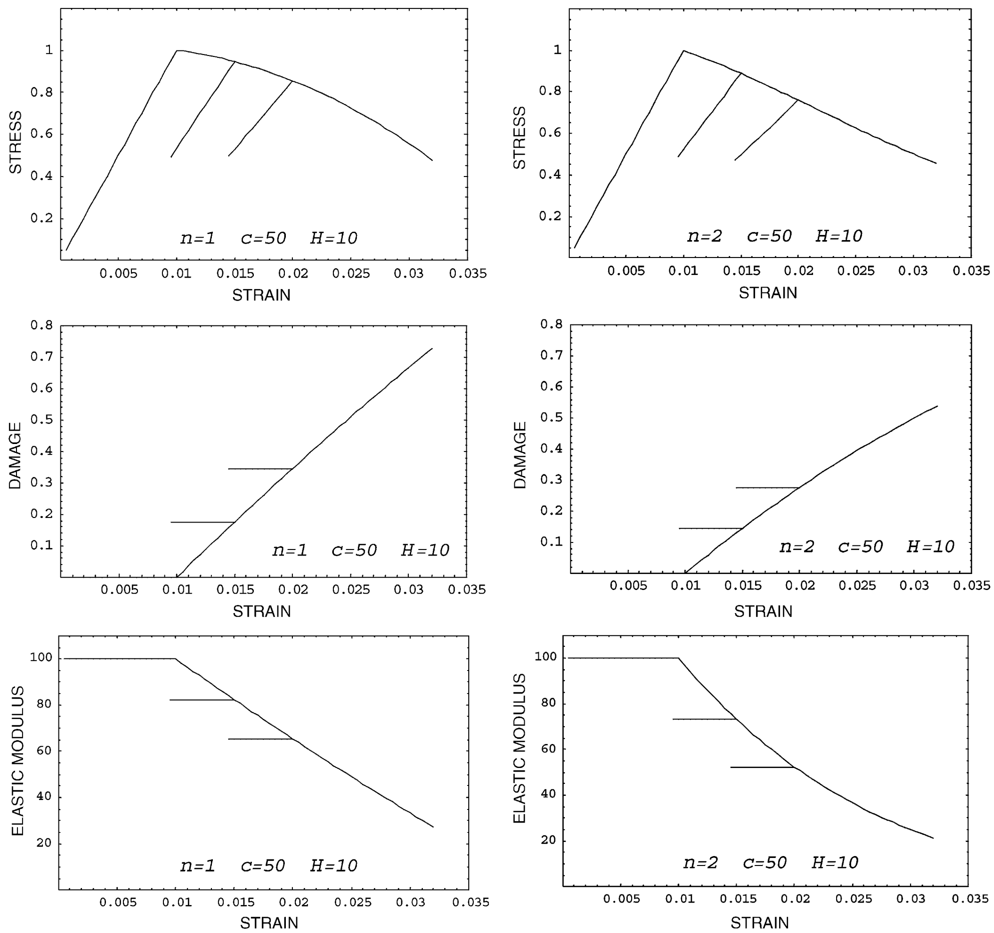

Fig. 10. Uniaxial processes for $n = 1, 2$, $c = 50$, $E = 100$. Mises criterion.

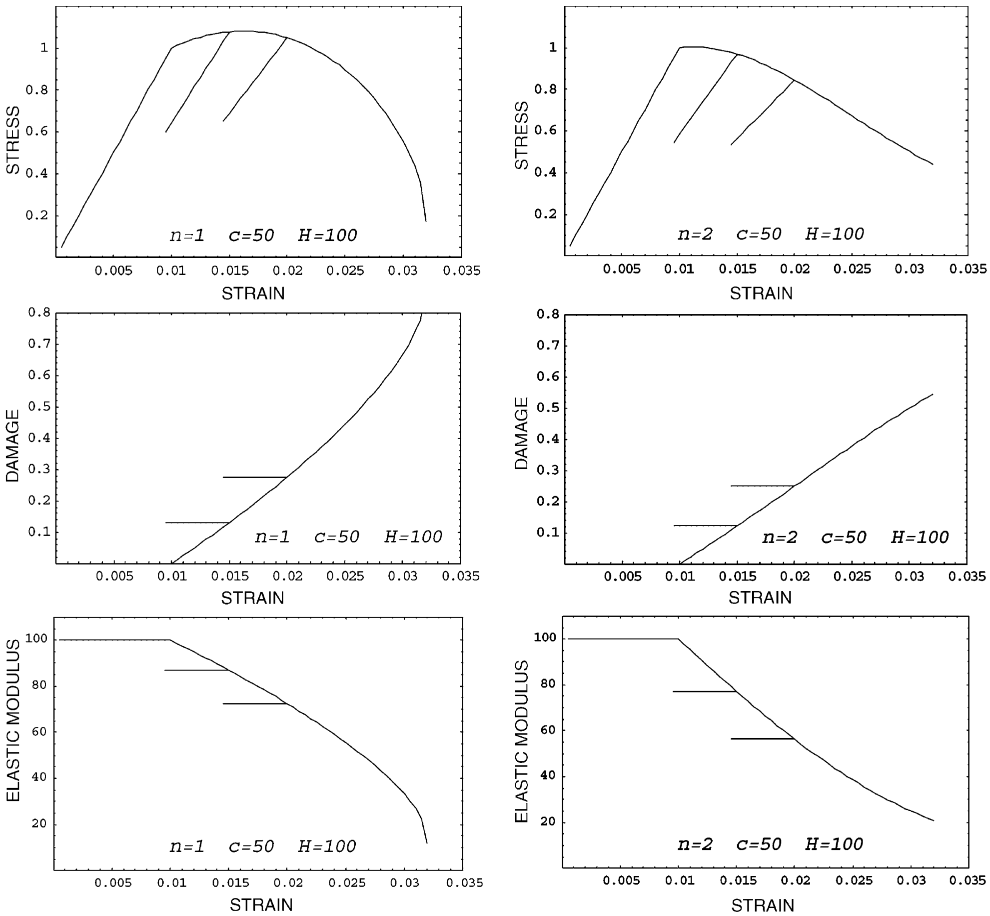

Fig. 11. Uniaxial processes for $n = 1$, 2, $c = 50$, $E = 100$. Mises criterion.

Figs. 10 and 11 refer to a loading–unloading uniaxial tensile process. In Fig. 10 the cases $n = 1$ and $n = 2$ are compared, for $c = 50$, $H = 10$, $\sigma_0 = 1$. The evolution of ω_p and of the elastic modulus E are also reported. Increasing values of n determine stronger reduction of the yield stress. The plots of Fig. 11 have been obtained for a very large value of H, thus comparable to the elastic stiffness, so that the tangent stiffness after first yield does not degrade immediately, as it has been observed in some experimental tests on concrete. Hardening then decreases fast as soon as damage develops, thanks to the coupling in the stored energy functional.

The parameters c and n particularly influence the degradation of the elastic modulus. The parameter n determines the concavity of the curve $E(\omega_e)$, that can be obtained from experiments (Fig. 12).

Similar considerations can be made in the case of cyclic uniaxial tension–compression processes. Fig. 13 illustrate the complete degradation of the elastic modulus E as ω_p ranges between 0 and 1.

A second group of examples concerns the Drucker-Prager criterion (57a) and (57b). The influence of the damage parameter c for $n = 2$ and two different hardening moduli on the uniaxial compression curve is presented in Figs. 14 and 15. It is evident that the model allows to simulate a continuous change from hardening to softening as well as the reduction in the stiffness. The influence of the hardening modulus is shown in Fig. 16.

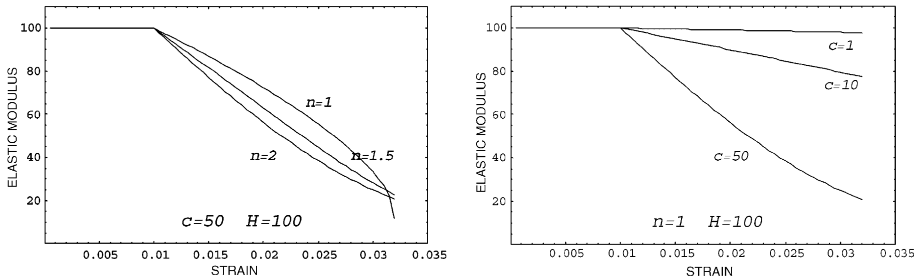

Fig. 12. Influence of the parameters n and c on the degradation of the elastic modulus E. Mises Criterion.

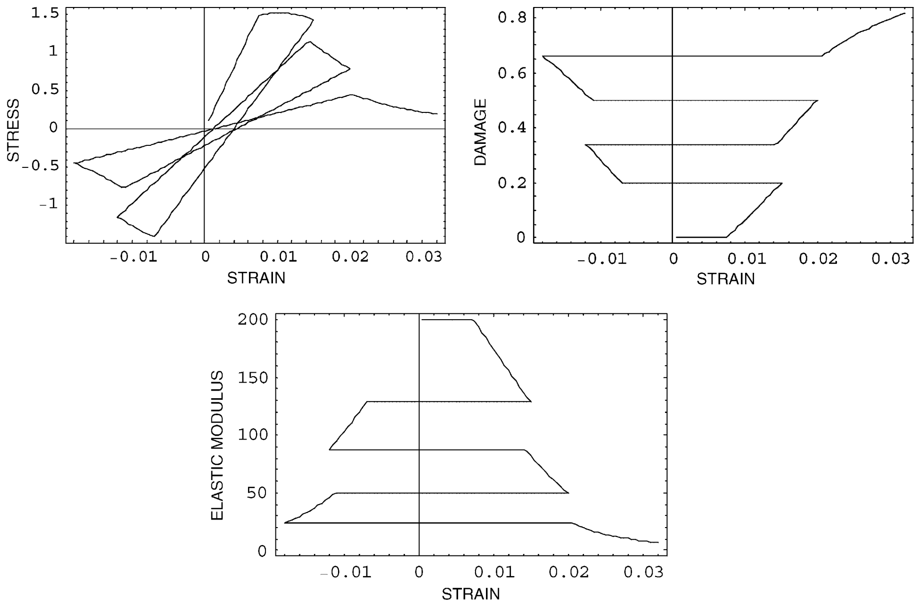

Fig. 13. Uniaxial cyclic process. $E = 200$, $H = 200$, $\sigma_0 = 2$, $n = 2$, $c = 50$. Mises criterion.

Fig. 17 concerns a panel subjected to shear. Three curves are reported. The middle one refers to Drucker-Prager criterion (57a) and (57b) with $y_c = 2.0$, $\xi = 10$. The top and bottom curves report the prediction of Mises criterion (56) with the same parameters and taking $\sigma_0 = y_c$ for the former, $\sigma_0 = y_t$ for the latter.

4.3. Multiaxial compression processes: comparison with experimental results

The predictions of the model examined in Section 4.2 are compared to experimental data obtained from tests on confined concrete (Van Mier, 1984). For monotonic loading and for relatively small values of the confinement pressure, the hypothesis of isotropic damage appears to be a reasonable approximation of the actual damage evolution. In order to avoid the occurrence of localisation, only the data in the hardening phase, before the peak, are used.

Let σ_1 be the major compressive stress. The confinement stresses σ_2 and σ_3 are assumed always compressive and proportional to the major stress: $\sigma_2 = k_1\sigma_1$, $\sigma_3 = k_2\sigma_1$.

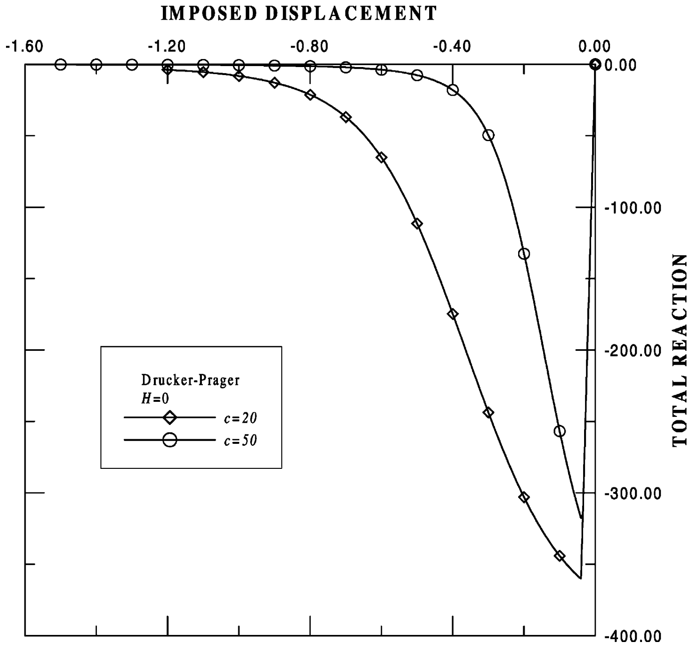

Fig. 14. Drucker-Prager-type criterion. Uniaxial monotonic compressive process. Variable c. $E = 36000$, $\nu = 0.3$, $H = 0$, $n = 2$, $\xi = 10$.

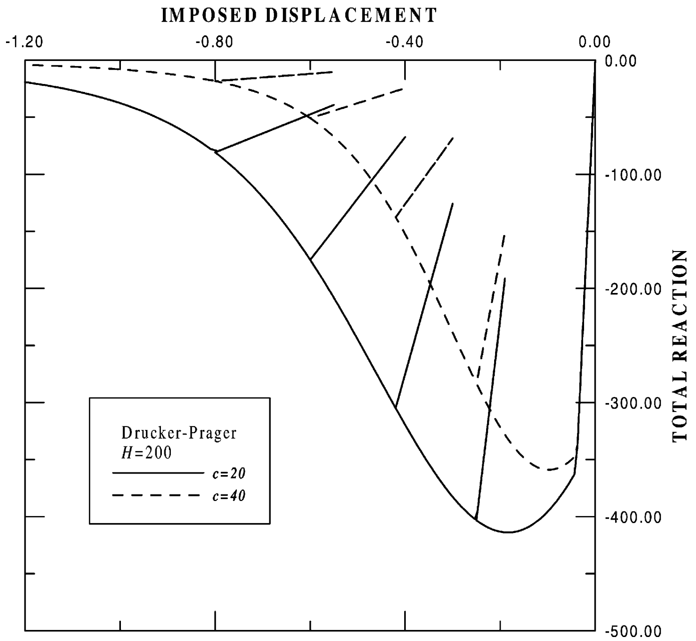

Fig. 15. Drucker-Prager-type criterion. Uniaxial cyclic compressive process. Variable c. $E = 36000$, $\nu = 0.3$, $H = 200$, $n = 2$, $\xi = 10$.

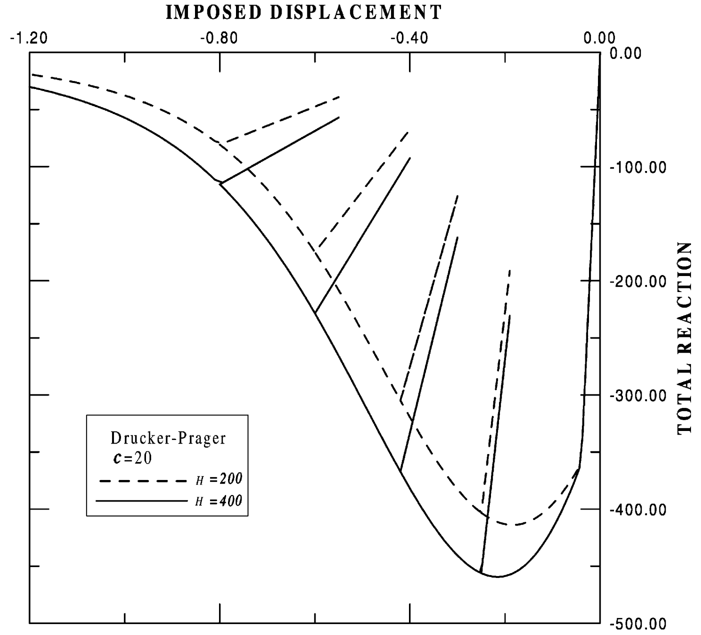

Fig. 16. Drucker-Prager-type criterion. Uniaxial cyclic compressive process. Variable H. $E = 36000$, $\nu = 0.3$, $n = 2$, $\xi = 10$.

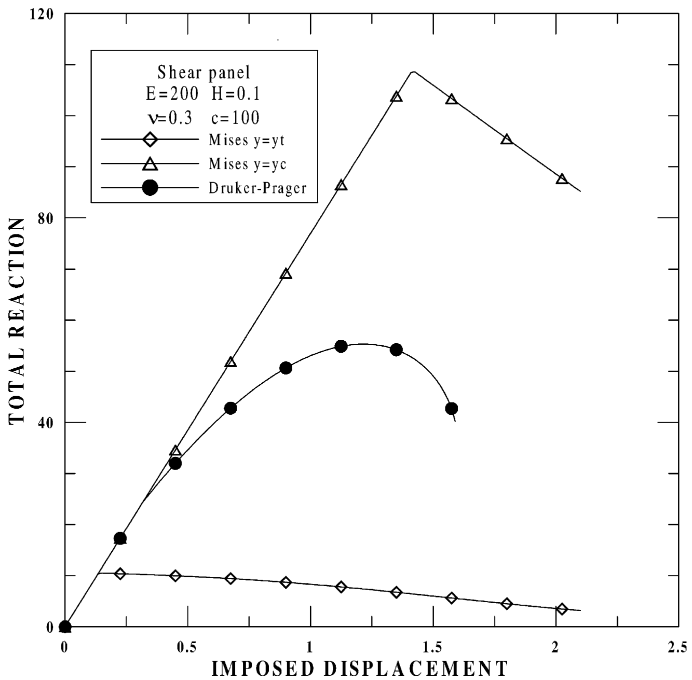

Fig. 17. Panel subject to shear. Comparison between Drucker-Prager and Mises criterion.

The yield function (57a) and (57b) reduces to:

$$g = \sqrt{\sigma_1^2(1 + k_1^2 + k_2^2 - k_1 - k_2 - k_1k_2)} + c\zeta - \chi - k_0 \leqslant 0 \tag{62}$$

$$\beta = 3\frac{\xi - 1}{\xi + 1} + 3\frac{cn}{2E_0}\frac{|y_c|}{\xi}\frac{(\xi^2 - 1)}{(\xi + 1)} \qquad k_0 = 2\frac{|y_c|}{\xi + 1} + \frac{cn}{2E_0}\frac{y_c^2}{\xi} \qquad \xi = \frac{|y_c|}{y_t}$$

Introducing the flow rules (41) and the constitutive equations (17) the following expressions relating the conjugated variables to the imposed stress are readily found:

$$\begin{aligned} \zeta &= \frac{n}{2E_0}\sigma_1^2[1 + k_1^2 + k_2^2 - 2v(k_1 + k_2 + k_1k_2)](1 + \omega_e)^{-(n+1)} + \frac{n_2}{2}H\frac{\omega_e^2}{c^2}(1 + \omega_e)^{n_2 - 1} \\ \chi &= -H\frac{\omega_e}{c}(1 + \omega_e)^{n_2} \qquad \omega_e \in [-1, 0] \end{aligned} \tag{63}$$

Note that in expressions (63) and (64) it has been used a different exponent n_2 for the damage law relative to the hardening modulus H.

Inserting (63) in (62) and solving the equation $g(\sigma_1, k_1, k_2, \omega_e) = 0$ for σ_1, the limit value of the major compressive stress σ_1 as function of ω_e and of the confinement ratios k_1 and k_2 is obtained:

$$\begin{aligned} \sigma_1 &= \frac{E_0(1 + \omega_e)^{n+1}}{Bcn}\left[A - \frac{1}{3}\beta C - \sqrt{\frac{2Bcn}{E_0(1 + \omega_e)^{n+1}}(k_0 - D) + \left(A - \frac{1}{3}\beta C\right)^2}\right] \\ A &= A(k_1, k_2) = \sqrt{1 + k_1^2 + k_2^2 - k_1 - k_2 - k_1k_2} \\ B &= B(k_1, k_2) = 1 + k_1^2 + k_2^2 - 2v(k_1 + k_2 + k_1k_2) \\ C &= C(k_1, k_2) = 1 + k_1 + k_2 \\ D &= D(\omega_e) = \frac{n_2}{2}H\frac{\omega_e^2}{c}(1 + \omega_e)^{n_2 - 1} - H\frac{\omega_e}{c}(1 + \omega_e)^{n_2} \end{aligned} \tag{64}$$

The corresponding limit value of the elastic deformation is obtained through the elastic condition

$$\varepsilon_1^{\lim} = \frac{(1 - vk_1 - vk_2)}{E_0(1 + \omega_e)^n}\sigma_1^{\lim} \tag{65}$$

The relation $\varepsilon_1^{\lim} - \sigma_1^{\lim}$, plotted in Figs. 18 and 19 for the uniaxial case, is obtained by eliminating ω_e from expressions (64) and (65) for fixed k_1, k_2. It is observed that the limit elastic strain and the limit elastic stress depend strongly on n and c. In Fig. 18 it has been assumed $c = 30$ while n takes the values 1, 1.5, 2. Fig. 19 refers to $n = 2$, while c takes the values 10, 50, 100. The values of n and c influence the value of the elastic strain for which the peak of the limit stress is reached.

Experimental data for a confined cyclic compression test on a concrete specimen is reported in Fig. 20. (Van Mier, 1984), from which the experimental relation $\varepsilon_1^{\lim} - \sigma_1^{\lim}$ has been derived for comparison with the prediction of the model given by Eq. (65). In this test the confinement pressures are given by the ratios $k_1 = 1/10$, $k_2 = 1/20$.

The constitutive parameters n and c have been obtained from the curve $E(\omega_e) - \varepsilon_1^{\lim}$ shown in Fig. 21. The parameter n, determined from the convexity of the curve, has been found equal to 2, while the parameter c has been determined, in lack of more specific data, by curve fitting. A good agreement with the experimental data can be obtained for $c = 70$. The comparison of the predicted relation $\varepsilon_1^{\lim} - \sigma_1^{\lim}$ with the experimental one is shown in Fig. 21. For values of ω_p larger than 0.15 softening appears in the experimental data (Fig. 22). The comparison between the envelope curve of the experimental test and the simulation of the model is shown in Fig. 23.

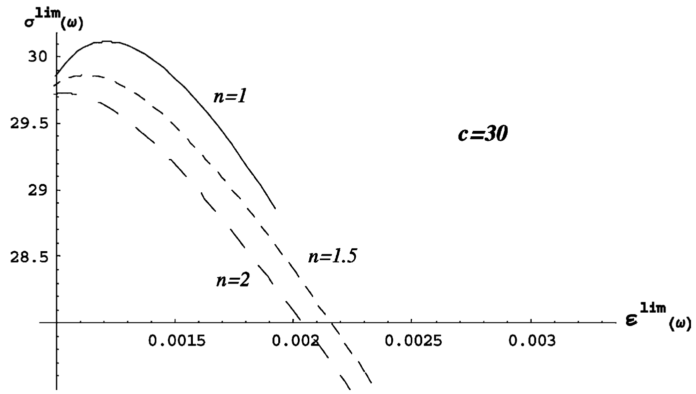

Fig. 18. Envelope of limit uniaxial elastic states for hardening isotropically damaged material. Constant *c*.

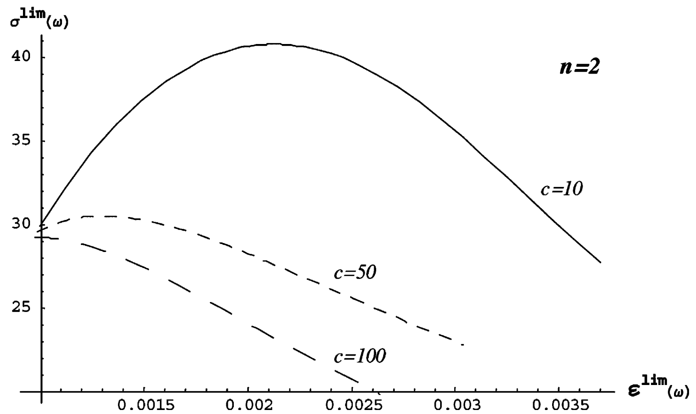

Fig. 19. Envelope of limit uniaxial elastic states for hardening isotropically damaged material. Constant *n*.

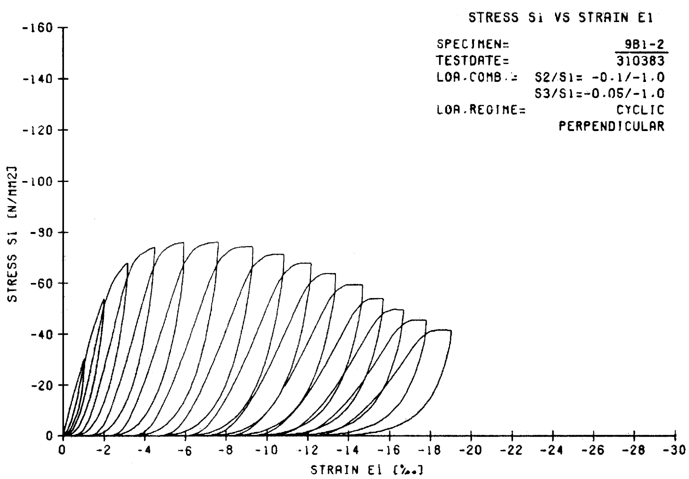

Fig. 20. Triaxial compressive stress–strain curve.

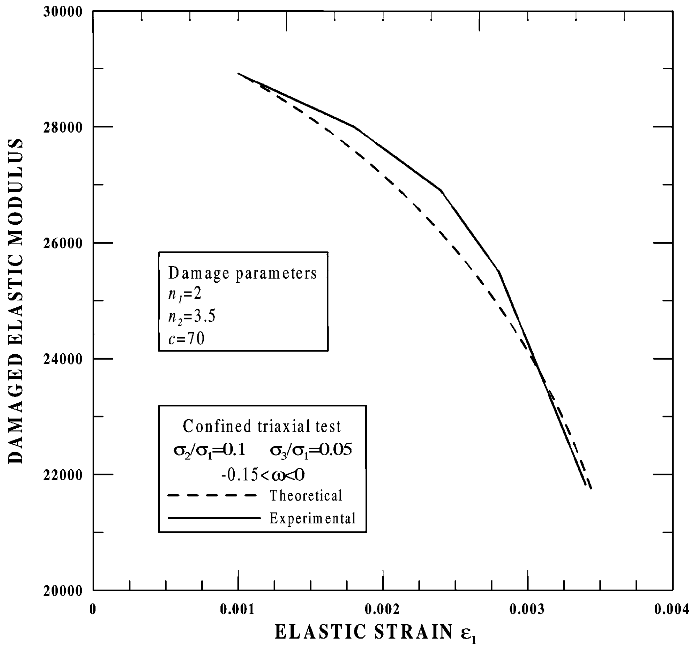

Fig. 21. Experimental degradation of the elastic modulus and model prediction for the test of Fig. 20.

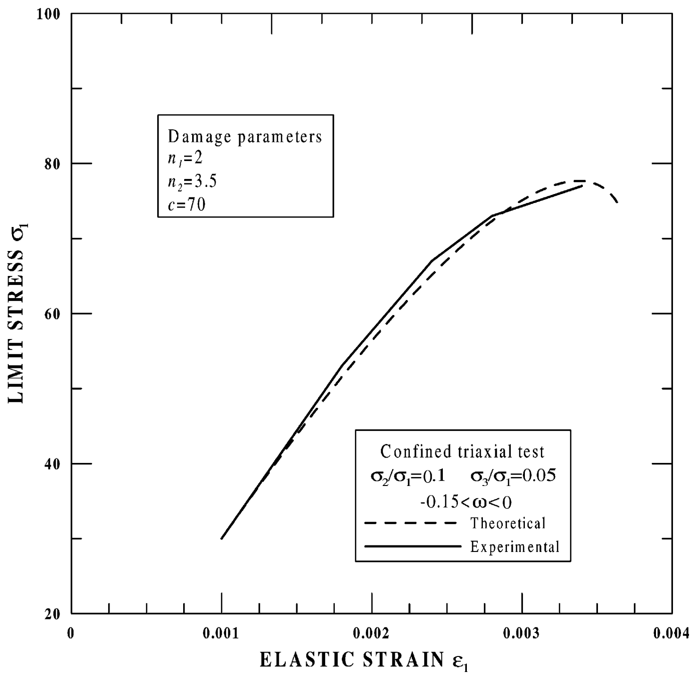

Fig. 22. Envelope of limit uniaxial elastic states. Comparison between experimental and theoretical data for the test of Fig. 20.

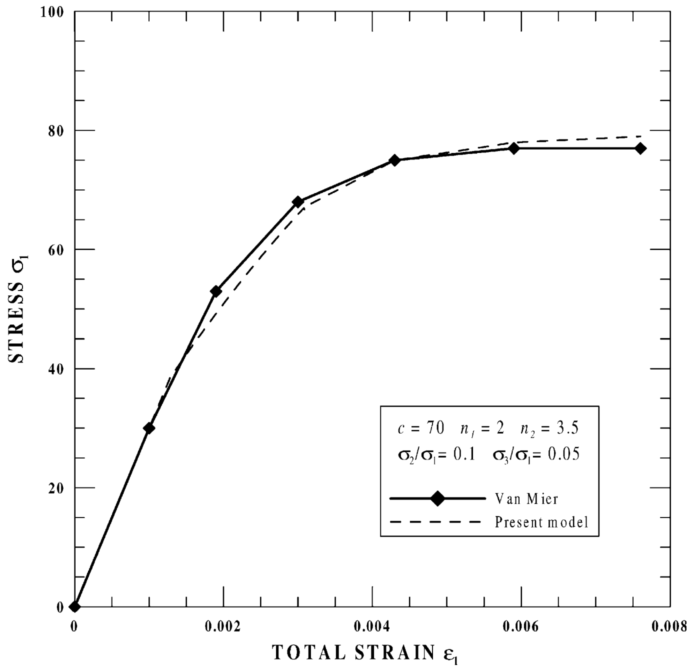

Fig. 23. Confined compressive test. Theoretical and experimental σ_1–ε_1 curves.

Table 1
Comparison of experimental and numerical value of the peak stress and elastic strain for confined compressive tests on concrete, $c = 70$; $n = 2$; $n_2 = 3.5$

k_1	k_2			
	0.05		0.1	
	Experimental	Theoretical	Experimental	Theoretical
0.33	$\sigma_{peak} = 83$ $\varepsilon_{peak} = 0.004$	$\sigma_{peak} = 89.7$ $\varepsilon_{peak} = 0.0041$	$\sigma_{peak} = 113$ $\varepsilon_{peak} = 0.0052$	$\sigma_{peak} = 95.64$ $\varepsilon_{peak} = 0.0043$
0.1	$\sigma_{peak} = 75$ $\varepsilon_{peak} = 0.0036$	$\sigma_{peak} = 77.6$ $\varepsilon_{peak} = 0.0034$	$\sigma_{peak} = 75$ $\varepsilon_{peak} = 0.0037$	$\sigma_{peak} = 80.9$ $\varepsilon_{peak} = 0.0036$

The model parameters c, n, n_2 so determined for the test of Fig. 20 have been used for numerically evaluating the peak value of the major stress and the corresponding elastic strain for different confinement pressure ratios. The results, presented in Table 1, are in reasonable agreement with the experimental data reported by Van Mier (1984).

5. Numerical algorithm

As it has been previously observed, the numerical implementation of the presented coupled plastic model is a generalisation of the standard algorithm for elastoplasticity with internal variables. In the context of a displacement FE method, at each iteration, given the predicted total deformation $\varepsilon + \Delta\varepsilon$, it can be found the algorithmic consistent tangent operator (Cuomo, submitted for publication)

$$\Phi^{ep}(\varepsilon) = \sup_{\tau}[\langle \eta, \tau \rangle - e^{c}(\tau) - d^{c}(\tau) - \langle \eta_{p}^{0}, \tau \rangle] \tag{66}$$

where the vector η_p^0 collects the values of accumulated irreversible kinematic variables at the beginning of the step.

It is examined the case of multiple constraints, where the yield surface is defined by (43). Here the complementary dissipation functional is given by any of the following expressions:

$$\begin{aligned} d^{c} &= \mathrm{In}K = \mathrm{In}\{\cap_{i=1,n}K_i\} = \sup_{\lambda_1 \geqslant 0} \ldots \sup_{\lambda_n \geqslant 0}\{\lambda_1 g_1(\tau) + \cdots + \lambda_n g_n(\tau)\} \\ &= \sup_{\lambda_1} \ldots \sup_{\lambda_n}\{\lambda_1 \bar{g}_1(\tau) + \cdots + \lambda_n \bar{g}_n(\tau)\} \end{aligned} \tag{67}$$

where μ is an arbitrary fixed positive (penalty) parameter and

$$\bar{g}_l = \max\left[g_i, -\frac{\lambda_i}{\mu}\right]\mu \in R \tag{68}$$

The second form of (67) derives from an augmented Lagrangian Regularisation (Bertsekas, 1982) that turns the inequality constraint $g_i \leqslant 0$ into the equality constraint $\bar{g}_l = 0$ and has several advantages. First of all, the Lagrangian multipliers are not limited in sign, moreover the gradients of the functions g_i are continuous in the neighbourhood of zero (Cuomo and Contrafatto, 2000a). This form is particularly useful in the case of corner points. The optimal value of the constant penalty parameter μ depends on the convexity properties of the problem.

The stationarity conditions of (66) are the compatibility and admissibility conditions:

$$\mathbf{r} = \begin{bmatrix} \varepsilon - \varepsilon_e - \varepsilon_{p_0} - \lambda_1 \nabla_\sigma \bar{g}_1 - \cdots - \lambda_l \nabla_\sigma \bar{g}_l \\ -\alpha_e - \alpha_{p_0} - \lambda_1 \nabla_\chi \bar{g}_1 - \cdots - \lambda_l \nabla_\chi \bar{g}_l \\ -\omega_e - \omega_{p_0} - \lambda_1 \nabla_\zeta \bar{g}_1 - \cdots - \lambda_l \nabla_\zeta \bar{g}_l \\ -\bar{g}_1 \\ \vdots \\ -\bar{g}_l \end{bmatrix} = \mathbf{0} \tag{69}$$

where l is the number of the constraints. The second and third rows of the residual vector (69) enforce the equality between the elastic and plastic parts of the internal variables, given by their respective constitutive equations (18a)–(18c) and (41).

The structure of the generic Newton's step for solving Eq. (69) is:

$$\left[\begin{array}{ccc|ccc} & & & \nabla_\sigma \bar{g}_1 & \cdots & \nabla_\sigma \bar{g}_l \\ & S_t^{-1} + \sum_{i=1,l} \lambda_i D_i & & \nabla_\chi \bar{g}_1 & \cdots & \nabla_\chi \bar{g}_l \\ & & & \nabla_\zeta \bar{g}_1 & \cdots & \nabla_\zeta \bar{g}_l \\ \hline \nabla_\sigma^T \bar{g}_1 & \nabla_\chi^T \bar{g}_1 & \nabla_\zeta^T \bar{g}_1 & \nabla_{\lambda_1} \bar{g}_1 & & \\ \vdots & \vdots & \vdots & & \ddots & \\ \nabla_\sigma^T \bar{g}_l & \nabla_\chi^T \bar{g}_l & \nabla_\zeta^T \bar{g}_l & & & \nabla_{\lambda_l} \bar{g}_l \end{array}\right] \begin{bmatrix} \delta\sigma \\ \delta\chi \\ \delta\zeta \\ \delta\lambda_1 \\ \vdots \\ \delta\lambda_l \end{bmatrix} = \mathbf{r}$$

where

$$S_t = \nabla^2_{\eta\eta} e(\eta(\tau)) \quad D_i = \begin{bmatrix} \nabla^2_{\sigma,\sigma}\bar{g}_l & \nabla^2_{\sigma,\chi}\bar{g}_l & \nabla^2_{\sigma,\zeta}\bar{g}_l \\ \nabla^2_{\chi,\sigma}\bar{g}_l & \nabla^2_{\chi,\chi}\bar{g}_l & \nabla^2_{\chi,\zeta}\bar{g}_l \\ \nabla^2_{\zeta,\sigma}\bar{g}_l & \nabla^2_{\zeta,\chi}\bar{g}_l & \nabla^2_{\zeta,\zeta}\bar{g}_l \end{bmatrix}$$

$$\nabla_\tau \bar{g}_i = \begin{cases} \nabla_\tau g_i & \text{if } g_i > -\frac{\lambda_i}{\mu} \\ 0 & \text{otherwise} \end{cases}$$

$$\nabla_{\lambda_i} \bar{g}_i = \begin{cases} 0 & \text{if } g_i > -\frac{\lambda_i}{\mu} \\ -\frac{1}{\mu} & \text{otherwise} \end{cases}$$

$$\nabla^2_{\tau\tau} \bar{g}_i = \begin{cases} \nabla^2_{\tau\tau} g_i & \text{if } g_i > -\frac{\lambda_i}{\mu} \\ 0 & \text{otherwise} \end{cases}$$

The procedure automatically guarantees the annihilation of the Lagrangian multipliers when a constraint switches from active to non-active. In the numerical implementation a reduced set of equations, including only the predicted active constraints, can be used. Note that the tangent operator is symmetric and it is a generalisation of the standard plasticity tangent operator, as opposite to the one found by other models (e.g. Hansen and Schreyer, 1994).

A structural application has been performed. The model has been applied to the extension of a rectangular strip with a hollow slit in the centre, a quarter of which is illustrated in Fig. 24. The coupled Mises criterion (56) has been used for the material with different values of the material constant c. Fig. 25 shows the total reaction versus the imposed vertical displacement for three different values of the damage parameter c ($c = 0$ is equivalent to absence of damage) in plane strain. The distribution of the equivalent stress J_2 is shown in Fig. 26 in plane stress conditions at the three different levels of stretching indicated in Fig. 27. Plastic deformations initially concentrate in the region near the tip of the slit and, as soon as damage occurs, migrate along the centreline, unloading the previously plasticised region.

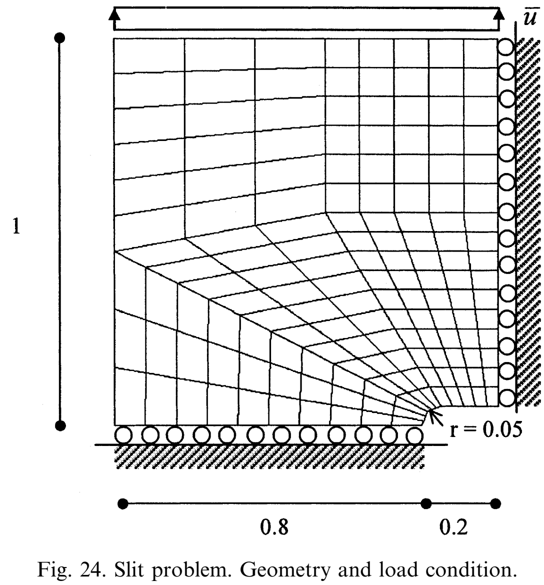

Fig. 24. Slit problem. Geometry and load condition.

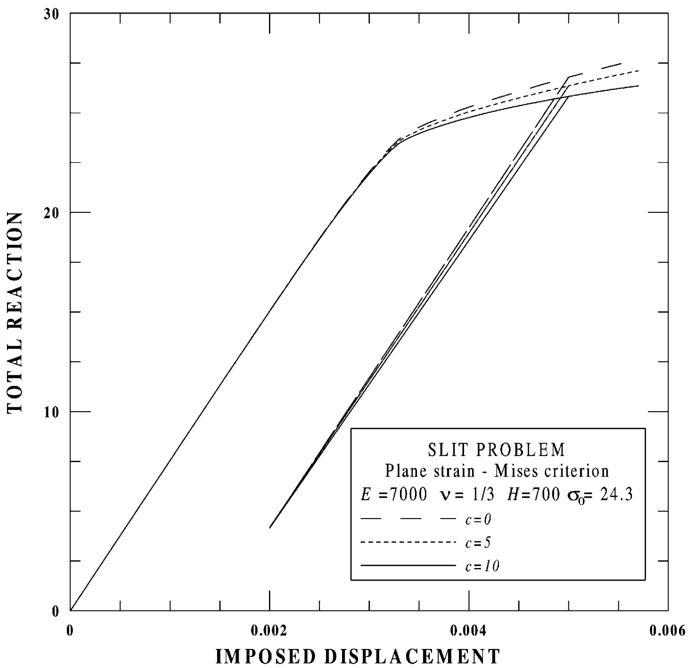

Fig. 25. Slit problem. Plane strain. Structural response for different values of the damage parameter c.

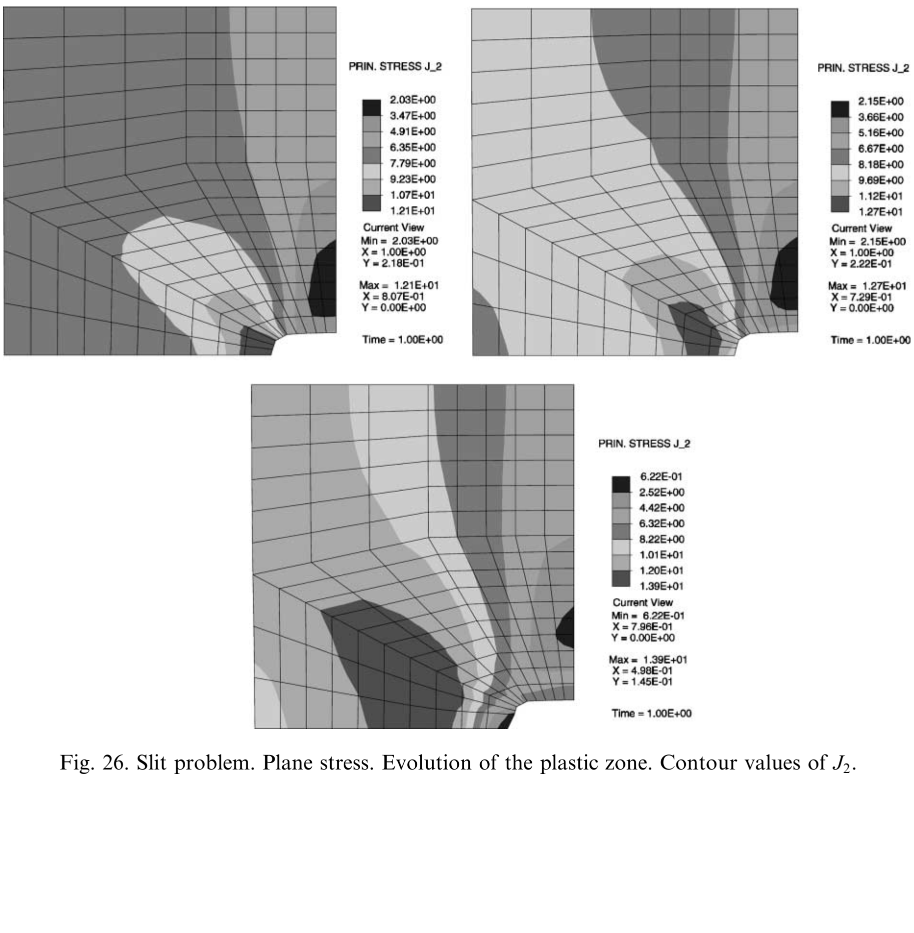

Fig. 26. Slit problem. Plane stress. Evolution of the plastic zone. Contour values of J_2.

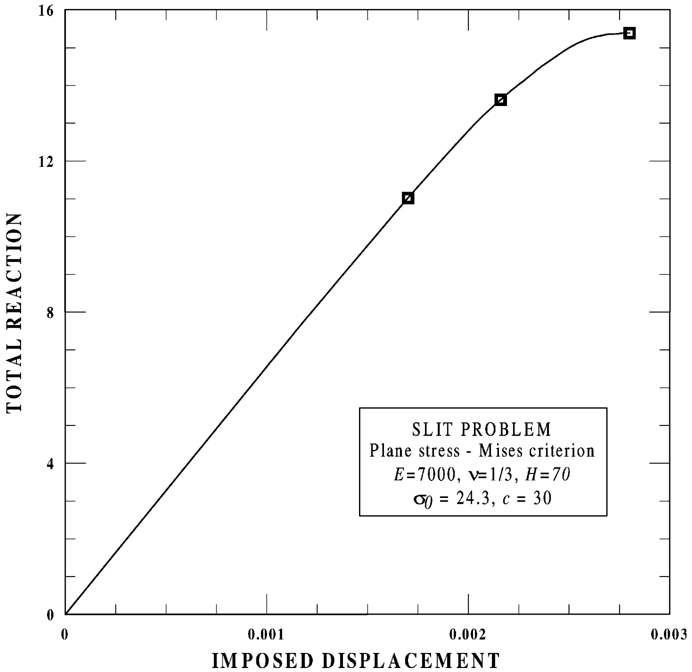

Fig. 27. Slit problem. Plane stress. Monotonic load condition.

6. Conclusions

An internal variable model of plasticity coupled with damage has been formulated in the framework of GSMM. It is based on the definition of the internal energy functional and of the dissipation potential, satisfying a priori the reduced dissipation inequality.

Various damaging material behaviours have been modelled, as plastic-hardening or cohesive fracture-like behaviour, depending on the choice of the dissipation functional, and therefore of the generalised elastic domain.

The model is completely formulated in the space of actual stresses and conjugated thermodynamic forces, avoiding the introduction of "effective" variables. The admissible domain is defined by means of a single potential. Consequently the evolution laws of any internal variable are obtained in a unified way.

A natural extension of Drucker's principle applies to the generalised elastic domain, so that the postulate of maximum dissipation is fulfilled. The satisfaction of the evolution laws is obtained solving a single optimisation problem, which turns out to be a straightforward generalisation of the one used in perfect plasticity. The model is associative and satisfies a generalised Drucker's postulate.

A particularisation of the model to the case of isotropic damage has been analysed. Because the constitutive evolution laws are derived as a consequence of energy balances, the damage coupling is based only on two material constants, which rule the rate and the concavity of the decay of the elastic modulus. These can be easily identified by means of usual experimental tests. It has been shown that the predictions of the model can reasonably simulate the experimental evolution of either damage in elastic-plastic materials or tests on confined concrete. Several mechanical behaviours have been modelled, both in monotonic and in cyclic processes. With the aid of a structural problem it has been shown the effectiveness of the numerical implementation of the model, that covers also the frequent case of multiple yield modes. The problem of strain localisation and mesh dependency, typical of damage models, has not been addressed in the paper, this aspect being under development in the framework of the proposed formulation.

Appendix A. Special functions

X, X' adjoint linear vector spaces
$\cdot\cdot$. dot product between tensor
$\langle\cdot,\cdot\rangle$ internal product
$\|\cdot\|$ Euclidean norm
$\bar{R} = R \cup \{+\infty\}$
Sub-differential of a functional

$$\forall f : S \subset X \to \bar{R} \quad \partial_x f(x,y) : S \to E' \subset X'$$
$$\partial_x f(x,y) = \{x' \in S' : f(\bar{x},y) - f(x,y) \geqslant \langle x', (\bar{x} - x)\rangle, \quad \forall \bar{x} \in S\}$$

Conjugated function

$$\forall f : S \subset X \to \bar{R} \quad f^{\mathrm{c}} : S' \to \bar{R} \quad f^{\mathrm{c}}(x') = \sup\{\langle x', x\rangle - f(x), \quad \forall x \in S\}$$

Fenchel's inequality

$$\forall f : S \subset X \to \bar{R} \quad \forall f^{\mathrm{c}} : S' \to \bar{R} \quad f(x) + f^{\mathrm{c}}(x') \leqslant \langle x', x\rangle \qquad (*)$$

If (*) holds with the equality the elements x and x' are conjugated and the following identities holds:

$$x \in \partial f'(x') \quad x' \in \partial f(x) \quad \langle x, x'\rangle = f(x) + f'(x')$$

Indicator function of a set S

$$\mathrm{In}K : X \to \bar{R} \quad \mathrm{In}K(x) \begin{cases} 0 & x \in K \\ +\infty & x \notin K \end{cases}$$

Support function of a set K

$$\mathrm{supp}\ K : X' \to \bar{R}\ \mathrm{supp}\ K(x') = \sup_x\{\langle x', x\rangle, x \in K\}$$

Relation between indicator function and support function of a set S

$$[\mathrm{In}K]^{\mathrm{c}}(x') = \sup_{x\in X}[\langle x, x'\rangle - \mathrm{In}K(x)] = \sup_{x\in K}[\langle x, x'\rangle] = [\mathrm{supp}K](x')$$

References

Armero, F., Oller, S., 2000. A general framework for continuum damage models, part I, II. Int. J. Solids Struct. 37, 7409–7464.
Bertsekas, D.P., 1982. Constrained Optimization and Lagrange Multiplier Methods. Academic Press, Boston.
Besseling, J.F., Van der Giessen, E., 1994. Mathematical Modelling of Inelastic Deformation. Chapman & Hall.
Borino, G., Fuschi, P., Polizzotto, C., 1996. Elastic–plastic-damage constitutive models with coupling internal variables. Mech. Res. Commun. 23, 19–28.
Chaboche, J.L., 1999. Thermodynamically founded CDM models for creep and other condition. In: Althenbach, H., Skrzypek J.J., (Eds.), Creep and Damage in Material Structures, CISM courses and lectures. n. 399.
Cordebois, J.P., Sidoroff, F., 1982. Endommagement anisotrope en elaticité et plasticité. J. Méc. Thé. App. Numéro spécial, 45–60.
Cuomo, M. Forms of the dissipation function for some classes of viscoplastic models, submitted to J. Plasticity.
Cuomo, M., Contrafatto, L., 2000a. Stress rate formulation for elastoplastic models with internal variables based on Augmented Lagrangian Regularisation. Int. J. Solids Struct. 37, 3935–3964.

Cuomo, M., Contrafatto, L., 2000b. On a thermodynamically consistent continuum model for concrete coupled with quasi-isotropic damage. In: Owen, D.R.J., Oñate, E., Hinton, E., (Eds.), European Congress on Computational Methods in Applied Sciences and Engineering, ECCOMAS 2000, Barcelona, 11–14 September, 2000.

Germain, P., 1973. Mécanique des Milieux Continus. Masson.

Halphen, B., Nguyen, Q.S., 1975. Sur les matériaux standards généralisés. J. de Mecanique 14, 39–63.

Hansen, N.R., Schreyer, H.L., 1994. A thermodinamically consistent framework for theories of elastoplasticity coupled with damage. Int. J. Solids Struct. 31 (3), 359–389.

Ju, J.W., 1989. On energy-based coupled elastoplastic damage theories: constitutive modelling and computational aspects. Int. J. Solids Struct. 25 (7), 803–833.

Kachanov, L.M., 1958. On the creep rupture time. Izv. Akad. Nauk SSSR, Otd. Tekhn. Nauk 8, 26–31.

Kluitenberg, G.A., 1962. On rheology and thermodinamic of irreversible processes. Physica 28, 561–568.

Krajcinovic, D., 1984. Continuum damage mechanics. Appl. Mech. Rev. 37 (1), 1–6.

Lemaitre, J., 1996. A Course on Damage Mechanics. Springer.

Lemaitre, J., Chaboche, J.L., 1985. Mécanique des Materiaux Solides. Dunod, Paris.

Marotti de Sciarra, F., 1997. A new variational theory and a computational algorithm for coupled elastoplastic damage models. Int. J. Solids Struct. 34, 1761–1796.

Klisinski, M., Mròz, Z., 1988. Description of inelastic deformation and degradation of concrete. Int. J. Solids Struct. 24 (4), 391–416.

Paas, M.H.J.W., Schreurs, P.J.G., Brekelmans, W.A.M., 1993. A continuum approach to brittle and fatigue damage: theory and numerical procedures. Int. J. Solids Struct. 30, 579–599.

Rockafellar, R.T., 1970. Convex Analysis. Princeton University Press, Princeton.

Romano, G., Rosati, L., Marotti de Sciarra, F., 1992. An internal variable theory of inelastic behaviour derived from uniaxial rigid perfectly plastic law. Int. J. Eng. Sci. 31 (8), 1105–1120.

Romano, G., Rosati, L., Marotti de Sciarra, F., 1993. A variational theory for finite-step elasto-plastic problems. Int. J. Solids Struct. 30, 2317–2334.

Simo, J.C., Ju, J.W., 1987. Stress and strain based continuum damage models, parts I and II. Int. J. Solids Struct. 23, 821–869.

Van Mier, J. G. M., 1984. Strain-softening of concrete under multiaxial loading condition, PhD Thesis, Eindhoven.

Zhu, Y.Y., Cescotto, S., 1995. A fully coupled elasto-viscoplastic damage theory for anisotropic materials. Int. J. Solids Struct. 32, 1607–1641.

Ziegler, H., 1977. An Introduction to Thermomechanics. In: Applied Mathematics and Mechanics 21. North-Holland Publishing Company.